ADJOINT-BASED OPTIMIZATION FOR RIGID BODY MOTION IN MULTIPHASE NAVIER-STOKES FLOW*

JULIA SPRINGER‡ AND KARSTEN URBAN§

Abstract. We consider the numerical simulation of rigid body motion in multiphase incompressible Navier-Stokes flow. The motion is formulated as an optimization problem and determined by minimizing an objective function in terms of forces and moments acting on the body, constrained by the multiphase Navier-Stokes equations. The corresponding adjoint system and boundary conditions are derived and derivatives of the objective function are determined. Numerical experiments include the flow around a NACA hydrofoil, a box and the standard benchmark KRISO Container Ship (KCS). We obtain a considerable speedup compared to current state-of-the-art methods.

Key words. Multiphase flow, incompressible Navier-Stokes equations, rigid body motion, adjoint methods

AMS subject classifications. 35Q35,76D05,76B75,70E15

1. Introduction. Computational Fluid Dynamics (CFD) has become a field of enormous importance both in research and in industry, [1, 7, 29]. The range of developments and applications is huge. We consider the numerical simulation of the motion of a rigid body in a two-phase flow, in particular the ship position in water for a given ship velocity. The position (or the motion) of the ship is determined by acting forces and moments. A standard numerical approach for rigid body motion reads as follows, [2, 32]:

1. Given an initial position of the ship, solve for velocity and pressure via the Navier-Stokes equations. Obtain forces and moments.
2. If the resulting forces and moments are balanced, stop.
3. Else: Determine the new position of the ship by solving the equations of motion based upon the forces and moments computed in 1.
4. Transform the computational mesh and go to 1.

Mathematically, the above approach is an iterative scheme based upon a fixed point method to find the balance of forces and moments that characterizes the position of the ship. It is well-known that such an approach may be extremely slow, which make it often unfeasible in real-world applications.

In this paper, we suggest a different approach. Since the position is determined by the *minimum* of acting forces and moments, this can be described as solving an optimization problem that is constrained by the Navier-Stokes equations. Solving such a pde-constrained method efficiently usually requires derivatives of the objective function (forces, moments) with respect to the parameter (ship position). Such derivatives are known to be computable by the adjoint approach, i.e., deriving first-order optimality conditions yielding a system of adjoint pde's.

Even though such an approach is in principle known and has been used in several (mostly academic) problems [5, 8, 12, 31], we are not aware of any paper considering the rigid body motion in a multiphase Navier-Stokes flow. The particular challenges are:

‡Voith Turbo Schneider Propulsion GmbH & Co. KG, Alexanderstr. 18, D-89522 Heidenheim, Germany, julia.springer@voith.com

§University of Ulm, Institute for Numerical Mathematics, Helmholtzstrasse 18, D-89069 Ulm, Germany, karsten.urban@uni-ulm.de

*This research was supported by Voith Turbo Schneider Propulsion, Heidenheim (Germany).

1. Derivation of the multiphase adjoint Navier-Stokes-system including a complete set of adjoint boundary conditions.
2. Computation of the derivative of the reduced objective function via transformation to a reference domain e.g. for a Newton-based optimization method.
3. Computation of the corresponding mesh transformations.
4. Efficient realization in software, simulation.

The current paper solves the above issues. Our final result is a detailed formulation of the corresponding problems combined with an efficient realization in the open source package OpenFOAM® [11]. It is validated on two academic test problems, namely the flow around a NACA hydrofoil and the flow around a box, where for the latter one also corresponding experiments have been performed, [27]. Finally, we consider a real-world application, namely the flow around the KRISO Container Ship (KCS) [18, 20], which is a widespread test case in ship engineering. We observe an enormous speedup, so that in the meantime we could perform similar computations for a wide class of real rigid bodies. More details can be found in [27].

The remainder of this paper is organized as follows. In Section 2, we describe our flow model, the incompressible multiphase Reynolds-Averaged Navier-Stokes equations, the equations of motion and the moving domain approach resulting in a nonlinear coupled system of pde's used for the computation of such problems so far. Section 3 is devoted to the detailed formulation and analysis of the pde-constrained optimization problem including the multiphase adjoint, the corresponding boundary conditions and the parameter derivatives. Our numerical results are shown in Section 4.

2. Flow Model. We aim at describing the flow model for rigid body motion. To this end, we consider different domains in order to suitably model the motion. Let $\Omega_{\text{ref}} \subset \mathbb{R}^d$, $d = 3$, be a fixed reference domain. The motion will later be fully described by a parameter $\boldsymbol{u} \in U$, where $U \subseteq \mathbb{R}^6$ (6 DOF, see below) is a finite-dimensional design space. This parameter $\boldsymbol{u}$ induces a domain mapping $\boldsymbol{u} \mapsto \boldsymbol{\tau}^{\boldsymbol{u}} : \mathbb{R}^3 \to \mathbb{R}^3$, so that the rigid body motion yields to a transformed flow domain

$$\Omega_{\boldsymbol{u}} := \boldsymbol{\tau}^{\boldsymbol{u}}(\Omega_{\text{ref}}).$$

We denote all variables w.r.t. the moving domain $\Omega_{\boldsymbol{u}}$ with tildes and those w.r.t. the reference domain Ω_{ref} without tildes.

2.1. Reynolds-Averaged Navier-Stokes Equations. We consider the well-known Reynolds-averaged Navier-Stokes (RANS) equations for incompressible, viscous, Newtonian fluids on a finite time interval $I := (0, T)$. Then, we look for the velocity $\tilde{\boldsymbol{v}} : \Omega_{\boldsymbol{u}} \times I \to \mathbb{R}^d$ and the pressure $\tilde{p} : \Omega_{\boldsymbol{u}} \times I \to \mathbb{R}$ satisfying

$$\partial_t \left(\tilde{\rho}\tilde{\boldsymbol{v}}\right) + \nabla\cdot \left(\tilde{\rho}\tilde{\boldsymbol{v}}\tilde{\boldsymbol{v}}^T\right) - \nabla\cdot \left(\tilde{\mu}_{\text{eff}} D(\tilde{\boldsymbol{v}})\right) + \nabla\tilde{p} = \tilde{\rho}\tilde{\boldsymbol{f}}, \qquad \text{on } \Omega_{\boldsymbol{u}} \times I, \tag{2.1a}$$

$$\nabla\cdot \tilde{\boldsymbol{v}} = 0, \qquad \text{on } \Omega_{\boldsymbol{u}} \times I, \tag{2.1b}$$

where $\tilde{\rho} : \Omega_{\boldsymbol{u}} \times I \to \mathbb{R}$ is the density, $\tilde{\mu}_{\text{eff}} : \Omega_{\boldsymbol{u}} \times I \to \mathbb{R}$ with $\tilde{\mu}_{\text{eff}}(\tilde{\boldsymbol{x}}, t) = \tilde{\mu} + \tilde{\mu}_T(\tilde{\boldsymbol{x}}, t)$ is the effective dynamic viscosity consisting of the dynamic viscosity constant $\tilde{\mu}$ and the turbulent dynamic viscosity $\tilde{\mu}_T(\tilde{\boldsymbol{x}}, t)$ and $\tilde{\boldsymbol{f}} : \Omega_{\boldsymbol{u}} \times I \to \mathbb{R}^d$ denotes the body forces. We abbreviate by $D(\tilde{\boldsymbol{v}}) := \nabla\tilde{\boldsymbol{v}} + \nabla\tilde{\boldsymbol{v}}^T$ the strain tensor. Moreover, we use ∂_t as a shorthand notation for the partial derivative w.r.t. time. We divide the boundary $\Gamma_{\boldsymbol{u}} := \partial\Omega_{\boldsymbol{u}}$ into disjoint parts $\Gamma_{\boldsymbol{u}} = \Gamma_{\boldsymbol{u},\text{in}} \cup \Gamma_{\boldsymbol{u},\text{out}} \cup \Gamma_{\boldsymbol{u},\text{nsl}}$, $\Gamma_{\boldsymbol{u},\text{nsl}} := \Gamma_{\boldsymbol{u},\text{B}} \cup \Gamma_{\boldsymbol{u},\text{wall}}$

(nsl: no-slip), and impose the following initial and boundary conditions

$$\tilde{\boldsymbol{v}}(\tilde{\boldsymbol{x}},0)=\tilde{\boldsymbol{v}}_0,\quad \tilde{p}(\tilde{\boldsymbol{x}},0)=\tilde{p}_0,\ \forall\tilde{\boldsymbol{x}}\in\Omega_{\boldsymbol{u}},\qquad\text{(initial)},\tag{2.1c}$$

$$\tilde{\boldsymbol{v}}(\tilde{\boldsymbol{x}},t)=0,\quad \tilde{\boldsymbol{n}}^T\nabla\tilde{p}(\tilde{\boldsymbol{x}},t)=0,\ \forall(\tilde{\boldsymbol{x}},t)\in\Gamma_{\boldsymbol{u},\mathrm{in}}\times I,\qquad\text{(inflow)},\tag{2.1d}$$

$$(\tilde{\boldsymbol{n}}\cdot\nabla)\tilde{\boldsymbol{v}}(\tilde{\boldsymbol{x}},t)=0,\quad \tilde{p}(\tilde{\boldsymbol{x}},t)=0,\ \forall(\tilde{\boldsymbol{x}},t)\in\Gamma_{\boldsymbol{u},\mathrm{out}}\times I,\qquad\text{(outflow)},\tag{2.1e}$$

$$\tilde{\boldsymbol{v}}(\tilde{\boldsymbol{x}},t)=0,\quad \tilde{\boldsymbol{n}}^T\nabla\tilde{p}(\tilde{\boldsymbol{x}},t)=0,\ \forall(\tilde{\boldsymbol{x}},t)\in\Gamma_{\boldsymbol{u},\mathrm{nsl}}\times I,\qquad\text{(wall, no-slip)}.\tag{2.1f}$$

where $\tilde{\boldsymbol{n}}:\partial\Omega_{\boldsymbol{u}}\times I\to\mathbb{R}^d$ denotes the outer unit normal at the domain boundary $\partial\Omega_{\boldsymbol{u}}$. The turbulent dynamic viscosity is evaluated using two-equation based turbulence models, namely the k-ε model [16] or the k-ω-SST model [19]. A detailed derivation of (2.1) can be found e.g. in [7].

2.2. Multiphase Flow. For multiphase flows, the different fluids are modeled via the Volume of Fluid (VOF) method [14]. This method is based upon a unique velocity and pressure function for both fluids where the different fluid areas are distinguished by an additional flow variable $\tilde{\alpha}:\Omega_{\boldsymbol{u}}\times I\to[0,1]$, called *volume fraction* or *phase fraction*, which is defined such that $\tilde{\alpha}(\tilde{\boldsymbol{x}},t)=1$ for areas occupied by fluid 1 (water) and $\tilde{\alpha}(\tilde{\boldsymbol{x}},t)=0$ for areas occupied by fluid 2 (air). The phase-averaged local fluid properties are then obtained by $\tilde{\rho}(\tilde{\boldsymbol{x}},t)=\tilde{\alpha}(\tilde{\boldsymbol{x}},t)\rho_1+(1-\tilde{\alpha}(\tilde{\boldsymbol{x}},t))\rho_2$ and $\tilde{\mu}(\tilde{\boldsymbol{x}},t)=\tilde{\alpha}(\tilde{\boldsymbol{x}},t)\mu_1+(1-\tilde{\alpha}(\tilde{\boldsymbol{x}},t))\mu_2$ with constant densities ρ_1 and ρ_2 and constant dynamic viscosities μ_1 and μ_2 corresponding to fluid 1 and fluid 2. The movement of the interface between water and air is determined via an additional scalar transport equation for the phase fraction variable $\tilde{\alpha}$ given by

$$\partial_t\tilde{\alpha}+\nabla\cdot(\tilde{\alpha}\tilde{\boldsymbol{v}})=0.\tag{2.2}$$

In order to model the two fluids as one continuum including surface tension forces in the momentum equation, the so-called *Continuum Surface Force* (CSF) model [3] is used assuming a transitional area of fixed thickness δ at the interface. In this area, $\tilde{\alpha}$ changes smoothly from zero to one, defined by a C^2-function. Hence, the surface tension effects can be modeled as a continuous volume force acting in the transitional area. The Navier-Stokes equations (2.1) thus become

$$\partial_t(\tilde{\rho}\tilde{\boldsymbol{v}})+\nabla\cdot(\tilde{\rho}\tilde{\boldsymbol{v}}\tilde{\boldsymbol{v}}^T)+\nabla\tilde{p}^*-\nabla\cdot(\tilde{\mu}_{\mathrm{eff}}D(\tilde{\boldsymbol{v}}))+\boldsymbol{g}^T\tilde{\boldsymbol{x}}\nabla\tilde{\rho}-\sigma\tilde{\kappa}\nabla\tilde{\alpha}=0,\ \text{on }\Omega_{\boldsymbol{u}}\times I,\tag{2.3a}$$

$$\nabla\cdot\tilde{\boldsymbol{v}}=0,\ \text{on }\Omega_{\boldsymbol{u}}\times I,\tag{2.3b}$$

$$\partial_t\tilde{\alpha}+\nabla\cdot(\tilde{\alpha}\tilde{\boldsymbol{v}})=0,\ \text{on }\Omega_{\boldsymbol{u}}\times I,\tag{2.3c}$$

$$\tilde{\boldsymbol{v}}(\cdot,0)=\tilde{\boldsymbol{v}}_0,\quad \tilde{p}^*(\cdot,0)=\tilde{p}_0^*,\quad \tilde{\alpha}(\cdot,0)=\tilde{\alpha}_0,\qquad\text{on }\Omega_{\boldsymbol{u}},\tag{2.3d}$$

$$\tilde{\boldsymbol{v}}=0,\quad \tilde{\boldsymbol{n}}^T\nabla\tilde{p}^*=0,\quad \tilde{\boldsymbol{n}}^T\nabla\tilde{\alpha}=0,\qquad\text{on }\Gamma_{\boldsymbol{u},\mathrm{nsl}}\times I,\tag{2.3e}$$

$$(\tilde{\boldsymbol{n}}\cdot\nabla)\tilde{\boldsymbol{v}}=0,\quad \tilde{p}^*=0,\quad \tilde{\boldsymbol{n}}^T\nabla\tilde{\alpha}=0,\qquad\text{on }\Gamma_{\boldsymbol{u},\mathrm{out}}\times I,\tag{2.3f}$$

$$\tilde{\boldsymbol{v}}=\tilde{\boldsymbol{v}}_{\mathrm{in}},\quad \tilde{\boldsymbol{n}}^T\nabla\tilde{p}^*=0,\qquad\text{on }\Gamma_{\boldsymbol{u},\mathrm{in}}\times I,\tag{2.3g}$$

$$\tilde{\alpha}=\tilde{\alpha}_{\mathrm{in}}(\boldsymbol{u})\qquad\text{on }\Gamma_{\boldsymbol{u},\mathrm{in}}\times I,\tag{2.3h}$$

where $\tilde{\mu}_{\mathrm{eff}}(\tilde{\boldsymbol{x}},t)=\tilde{\alpha}(\tilde{\boldsymbol{x}},t)\mu_1+(1-\tilde{\alpha}(\tilde{\boldsymbol{x}},t))\mu_2+\tilde{\mu}_T(\tilde{\boldsymbol{x}},t)$ denotes the phase-averaged effective dynamic viscosity, $\tilde{\kappa}:\Omega_{\boldsymbol{u}}\times I\to\mathbb{R}$ is the curvature at the interface and σ is the surface tension coefficient. Moreover, $\tilde{p}^*:\Omega_{\boldsymbol{u}}\times I\to\mathbb{R}$ is the pressure part remaining when subtracting the hydrostatic pressure $\tilde{p}_{\mathrm{hydro}}=\tilde{\rho}\boldsymbol{g}^T\tilde{\boldsymbol{x}}$ from the total pressure $\tilde{p}$, i.e. $\tilde{p}=\tilde{p}^*+\tilde{\rho}\boldsymbol{g}^T\tilde{\boldsymbol{x}}$ (where an initial free surface location at $\tilde{\boldsymbol{x}}_3=0$ is assumed). Thus, (2.3a-2.3c) are coupled differential equations, (2.3e-2.3h) are boundary conditions and (2.3d) is the initial condition. As for the optimization we consider static positions with static flow fields, the time dependency is only kept for numerical reasons. Hence, the adjoint system is derived starting from the *stationary* system which corresponds to the converged (w.r.t. time) primal solution and reads:

$$
\begin{aligned}
&(2.4a) && \nabla\cdot\left(\tilde\rho\tilde{\boldsymbol v}\tilde{\boldsymbol v}^T\right)+\nabla\tilde p^*-\nabla\cdot\left(\tilde\mu_{\text{eff}}D(\tilde{\boldsymbol v})\right)+\boldsymbol g^T\boldsymbol x_{\text{init}}\nabla\tilde\rho=0, && \text{on } \Omega_{\boldsymbol u},\\
&(2.4b) && \nabla\cdot\tilde{\boldsymbol v}=0, && \text{on } \Omega_{\boldsymbol u},\\
&(2.4c) && \nabla\cdot(\tilde\alpha\tilde{\boldsymbol v})=0, && \text{on } \Omega_{\boldsymbol u},\\
&(2.4d) && \tilde{\boldsymbol v}=0,\quad \tilde{\boldsymbol n}^T\nabla\tilde p^*=0,\quad \tilde{\boldsymbol n}^T\nabla\tilde\alpha=0, && \text{on } \Gamma_{\boldsymbol u,\text{nsl}},\\
&(2.4e) && (\tilde{\boldsymbol n}\cdot\nabla)\,\tilde{\boldsymbol v}=0,\quad \tilde p^*=0,\quad \tilde{\boldsymbol n}^T\nabla\tilde\alpha=0, && \text{on } \Gamma_{\boldsymbol u,\text{out}},\\
&(2.4f) && \tilde{\boldsymbol v}=\tilde{\boldsymbol v}_{\text{in}},\quad \tilde{\boldsymbol n}^T\nabla\tilde p^*=0, && \text{on } \Gamma_{\boldsymbol u,\text{in}},\\
&(2.4g) && \tilde\alpha-\tilde\alpha_{\text{in}}(\boldsymbol u)=0, && \text{on } \Gamma_{\boldsymbol u,\text{in}}.
\end{aligned}
$$

We define the space of physical variables with admissible boundary conditions as

$$(2.5)\quad Y(\Omega_{\boldsymbol u}) := \{\tilde{\boldsymbol y}=(\tilde{\boldsymbol v},\tilde p^*\tilde\alpha)\in \boldsymbol V(\text{div})\times L_2(\Omega_{\boldsymbol u})\times L_2(\Omega_{\boldsymbol u}) : (2.4\text{d})-(2.4\text{f})\ \text{ hold}\},$$

where $\boldsymbol V(\text{div}) := \{\tilde{\boldsymbol w}\in \boldsymbol H^1(\Omega_{\boldsymbol u})^d : \nabla\cdot\tilde{\boldsymbol w}=0\}$. Note, that $Y(\Omega_{\boldsymbol u})$ does not involve the inflow condition (2.4g) for the phase variable $\tilde\alpha$ since this condition is parameter-dependent due to the domain transformation. Next, we collect the solution to (2.4) in one vector $\tilde{\boldsymbol y} := (\tilde{\boldsymbol v},\tilde p^*,\tilde\alpha)$, define the operator $\bar{\mathcal R} : Y(\Omega_{\boldsymbol u})\times U \to Z(\Omega_{\boldsymbol u})$ with $Z(\Omega_{\boldsymbol u}) := Y(\Omega_{\boldsymbol u})^*\times L_2(\Gamma_{\boldsymbol u,\text{in}})$ as

$$(2.6)\qquad \bar{\mathcal R}(\tilde{\boldsymbol y},\boldsymbol u)=0 \quad :\Longleftrightarrow\ \tilde{\boldsymbol y}\ \text{solves}\,(2.4\text{a})-(2.4\text{c}),(2.4\text{g})\ \text{ in variational form}$$

and denote the solution as $\tilde{\boldsymbol y}(\boldsymbol u)$ in order to keep track of the dependency on the parameter $\boldsymbol u$. Note, that $\bar{\mathcal R}(\tilde{\boldsymbol y},\boldsymbol u)=0$ means that (2.4a)-(2.4c), (2.4g) are tested with a vector $\tilde{\boldsymbol\lambda}=(\tilde{\boldsymbol w},\tilde q,\tilde\gamma,\tilde\gamma_{\text{in}})\in Z(\Omega_{\boldsymbol u})^*$.

2.3. Time-Resolved Rigid Body Motion. The motion of a ship floating in water is enforced by the forces and moments acting on the surface of the rigid body. It turns out that the rigid body motion computations can be separated into two independent sub-problems for translation and rotation only by considering two different coordinate systems. In this section, we also recall the standard numerical scheme for determining rigid body motion by using the equations of motion and determining the evolutionary effect of forces and moments acting on the rigid body.

2.3.1. Frames of Reference. We may neglect deformations of the ship hull. Thus, the rigid body motion can be fully described by its components corresponding to six directions. These directions consist of three translations in the three coordinate directions and three rotations around the axes, which results in a total of six degrees of freedom (6 DOF). In the context of ship or aircraft movements, the motion directions for the translations are called *surge* (Δx), *sway* (Δy) and *sinkage* or *heave* (Δz). The motion directions for the rotation described as Euler angles are called *roll* or *heel* (ϕ), *pitch* or *trim* (θ) and *yaw* or *drift* (ψ). Since the rotation angles are not commutative, a consistent order of the rotations is crucial, see e.g. [2, 32]. Alternative descriptions can be done e.g. by an orientation matrix or by quaternions. For the description of the body motion two different frames of reference are used, in particular this is a *global coordinate system* that is moving forward with the constant ship speed and a *body-fixed coordinate system* with origin in the center of gravity which moves according to the body motion.

2.3.2. Rigid Body Motion Equations. The governing equations are determined by the variations of the linear and angular momentum. For the translation, we use that the variation of the linear momentum is equal to the acting forces

$$\partial_t \left(m \boldsymbol{v}_G \right) = \tilde{\boldsymbol{f}}, \quad \text{i.e.} \quad m \ddot{\boldsymbol{x}}_G = \tilde{\boldsymbol{f}}, \tag{2.7}$$

where m is the body mass, $\tilde{\boldsymbol{f}}$ the force vector, $\boldsymbol{v}_G = \dot{\boldsymbol{x}}_G$ the velocity and $\ddot{\boldsymbol{x}}_G$ the acceleration of the center of gravity $\boldsymbol{x}_G$. The total force $\tilde{\boldsymbol{f}}$ consists of surface forces $\tilde{\boldsymbol{f}}_{\text{flow}}$, field forces $\tilde{\boldsymbol{f}}_{\text{field}}$ and external forces $\boldsymbol{f}_{\text{ext}}$. The surface forces are the static and dynamic flow forces of water and air flow acting on the body. They can be calculated by integrating pressure and shear forces acting on the body surface. In most applications, gravity is the only acting field force. External forces can be e.g. towing forces that act on a specific point $\tilde{\boldsymbol{x}}_{\text{ext}} \in \Gamma_{\boldsymbol{u},\text{B}}$. The total forces read

$$\begin{aligned} \tilde{\boldsymbol{f}} \left(\left(\tilde{\boldsymbol{v}}, \tilde{p}^*, \tilde{\alpha} \right), \boldsymbol{u} \right) &= \int_{\Gamma_{\boldsymbol{u},\text{B}}} \left\{ \left(\tilde{p}^* + \tilde{\rho} \boldsymbol{g}^T \boldsymbol{x} \right) \boldsymbol{I} - \tilde{\mu}_{\text{eff}} D(\tilde{\boldsymbol{v}}) \right\} \tilde{\boldsymbol{n}} \, \mathrm{d}S + m\boldsymbol{g} + \boldsymbol{f}_{\text{ext}}, \\ &=: \tilde{\boldsymbol{f}}_{\text{flow}}(\tilde{\boldsymbol{y}}, \boldsymbol{u}) + \boldsymbol{f}_{\text{fix}}, \qquad \boldsymbol{f}_{\text{fix}} := m\boldsymbol{g} + \boldsymbol{f}_{\text{ext}}, \end{aligned} \tag{2.8}$$

where $\boldsymbol{I}$ is the unit tensor and $\tilde{\mu}_{\text{eff}} D(\tilde{\boldsymbol{v}})$ the viscous stress tensor. Then, by integrating (2.7) w.r.t. time we obtain $\dot{\boldsymbol{x}}_G$ and another integration w.r.t. time yields the position $\boldsymbol{x}_G$. For determining the rotations we use the relation that the variation of angular momentum w.r.t. $\boldsymbol{x}_G$ is equal to the acting moments:

$$\partial_t \left(\boldsymbol{I}_G \boldsymbol{\omega}_G \right) = \tilde{\boldsymbol{m}}, \qquad \text{where} \quad \boldsymbol{I}_G := \begin{pmatrix} \boldsymbol{I}_{xx} & -\boldsymbol{I}_{xy} & -\boldsymbol{I}_{xz} \\ -\boldsymbol{I}_{yx} & \boldsymbol{I}_{yy} & -\boldsymbol{I}_{yz} \\ -\boldsymbol{I}_{zx} & -\boldsymbol{I}_{zy} & \boldsymbol{I}_{zz} \end{pmatrix}, \tag{2.9}$$

i.e., $\boldsymbol{I}_G$ is the inertia tensor described in terms of the global coordinate system, $\tilde{\boldsymbol{m}}$ is the moment vector and $\boldsymbol{\omega}_G$ is the angular velocity. Note that the equations of motion for rotation need to be described in terms of the global coordinate system. Therefore, $\boldsymbol{I}_G$ is time dependent and we use transformations between the coordinate systems in order to describe $\boldsymbol{I}_G$ in terms of $\boldsymbol{I}_B$, which is the inertia tensor with respect to the body-fixed coordinate system and thus constant in time. For the transformation, we use the matrix T of the body fixed system. This allows us to write (2.9) as $T\boldsymbol{I}_B T^T \dot{\boldsymbol{\omega}}_G + \boldsymbol{\omega}_G \times T\boldsymbol{I}_B T^T \boldsymbol{\omega}_G = \tilde{\boldsymbol{m}}$, i.e.,

$$\dot{\boldsymbol{\omega}}_G = T\boldsymbol{I}_B^{-1} T^T \left(\tilde{\boldsymbol{m}} - \boldsymbol{\omega}_G \times T\boldsymbol{I}_B T^T \boldsymbol{\omega}_G \right), \tag{2.10}$$

where $\dot{\boldsymbol{\omega}}_G$ is the angular acceleration. The moments $\tilde{\boldsymbol{m}}$ acting on the body are determined similar to the forces, but contain an additional multiplication with the lever arm $(\tilde{\boldsymbol{x}} - \tilde{\boldsymbol{x}}_G)$ via cross product, i.e.,

$$\begin{aligned} &\tilde{\boldsymbol{m}} \left(\left(\tilde{\boldsymbol{v}}, \tilde{p}^*, \tilde{\alpha} \right), \boldsymbol{u} \right) =: \tilde{\boldsymbol{m}}_{\text{flow}} \left(\tilde{\boldsymbol{y}}, \boldsymbol{u} \right) + \tilde{\boldsymbol{m}}_{\text{fix}} = \\ &= \int_{\Gamma_{\boldsymbol{u},\text{B}}} (\tilde{\boldsymbol{x}} - \tilde{\boldsymbol{x}}_G) \times \{ [(\tilde{p}^* + \tilde{\rho}(\tilde{\alpha}) \boldsymbol{g}^T \tilde{\boldsymbol{x}}) \boldsymbol{I} - \tilde{\mu}_{\text{eff}}(\tilde{\alpha}) D(\tilde{\boldsymbol{v}})] \tilde{\boldsymbol{n}} \} \mathrm{d}S + (\tilde{\boldsymbol{x}}_{\text{ext}} - \tilde{\boldsymbol{x}}_G) \times \boldsymbol{f}_{\text{ext}}, \end{aligned} \tag{2.11}$$

where $\tilde{\boldsymbol{m}}_{\text{fix}} = \tilde{\boldsymbol{m}}_{\text{ext}} = (\tilde{\boldsymbol{x}}_{\text{ext}} - \tilde{\boldsymbol{x}}_G) \times \boldsymbol{f}_{\text{ext}}$ contains the external moments. By integration of (2.10) in time we get $\boldsymbol{\omega}_G$ and a second integration yields the orientation.

Equations (2.7) and (2.10) build a system of second-order ordinary differential equations. In the case of translations, (2.7) can be solved as three independent scalar differential equations which each can be transformed into a system of first order ordinary differential equations. In the case of rotations this is in general not possible as the rotations are strongly coupled if more than one rotational direction is considered. Therefore the rotational equations have to be solved as one system. Due to the specific structure of the equations, we use the well-known leapfrog integration, [27].

2.3.3. Moving Domains. Due to the body motions the flow domain changes in time. Hence, for dynamic computations we use the Arbitrary Lagrangian Eulerian (ALE) formulation of the momentum equation (see e.g. [13]), which corrects the convective term with the actual motion velocity $\tilde{\boldsymbol{v}}_m$ of the domain $\nabla\cdot\left(\tilde{\rho}\left(\tilde{\boldsymbol{v}}-\tilde{\boldsymbol{v}}_m\right)\tilde{\boldsymbol{v}}^T\right)$. For all other equations the same correction has to be applied to the convective term.

There are several approaches to determine the motion or distortion of the computational domain enforced by the rigid body motion, e.g. the whole-grid method, motion of the object boundary $\Gamma_{\boldsymbol{u},\mathrm{B}}$ only or various versions of deformation strategies like transfinite element mappings [9, 10] or a Laplace equation based mapping [30, 33], which has been used here.

3. Constrained Optimization for Rigid Body Motion. As already explained earlier, we wish to determine the position of the rigid body (here a ship) in terms of the minimum of forces defined in (2.8) and moments detailed in (2.11). We combine them in a single objective function by using appropriate weighting factors $a_f, a_m \in \mathbb{R}^+$ and matrices $\Theta_f, \Theta_m \in \mathbb{R}^{d\times d}$ to select the components of interest

$$\bar{\mathcal{J}}(\tilde{\boldsymbol{y}},\boldsymbol{u}) := a_f\|\Theta_f^T\tilde{\boldsymbol{f}}\left(\tilde{\boldsymbol{y}},\boldsymbol{u}\right)\|_2^2 + a_m\|\Theta_m^T\tilde{\boldsymbol{m}}\left(\tilde{\boldsymbol{y}},\boldsymbol{u}\right)\|_2^2, \tag{3.1}$$

recalling $\tilde{\boldsymbol{y}} = (\tilde{\boldsymbol{v}}, \tilde{p}^*, \tilde{\alpha})$. We also use the multidimensional function $\bar{\boldsymbol{\mathcal{J}}}\left(\tilde{\boldsymbol{y}},\boldsymbol{u}\right) : Y(\Omega_{\boldsymbol{u}})\times U \to \mathbb{R}^{2d}$ defined as $\bar{\boldsymbol{\mathcal{J}}}(\tilde{\boldsymbol{y}},\boldsymbol{u}) := (\Theta_m^T\tilde{\boldsymbol{m}}\left(\tilde{\boldsymbol{y}},\boldsymbol{u}\right), \Theta_f^T\tilde{\boldsymbol{f}}\left(\tilde{\boldsymbol{y}},\boldsymbol{u}\right))^T$. Using the latter turns the optimization problem into finding roots of $\bar{\boldsymbol{\mathcal{J}}}$, which will be used for the efficient numerical solution in Section 4 below. For details, we refer to [27].

A closer look to (2.8) and (2.11) shows that the functional $\bar{\mathcal{J}}_{\mathrm{RBM}}$ for the specific case of the rigid body motion consists only of a body-related part acting only on the boundary $\Gamma_{\boldsymbol{u},\mathrm{B}}$, i.e.,

$$\bar{\mathcal{J}}_{\mathrm{RBM}}\left(\tilde{\boldsymbol{y}},\boldsymbol{u}\right) := \bar{\mathcal{J}}^{\Gamma_{\boldsymbol{u},\mathrm{B}}}\left(\tilde{\boldsymbol{y}},\boldsymbol{u}\right) = \int_{\Gamma_{\boldsymbol{u},\mathrm{B}}} \hat{\mathcal{J}}^{\partial\Omega}\left(\tilde{\boldsymbol{y}},\boldsymbol{u}\right)\mathrm{d}\boldsymbol{x}. \tag{3.2}$$

At this point, we wish to keep the considerations slightly more general by allowing contributions in the objective functions on all of $\Omega_{\boldsymbol{u}}$ and $\Gamma_{\boldsymbol{u}}$, i.e.,

$$\bar{\mathcal{J}}\left(\tilde{\boldsymbol{y}},\boldsymbol{u}\right) := \bar{\mathcal{J}}^{\partial\Omega}\left(\tilde{\boldsymbol{y}},\boldsymbol{u}\right) + \bar{\mathcal{J}}^{\Omega}\left(\tilde{\boldsymbol{y}},\boldsymbol{u}\right) = \int_{\partial\Omega_{\boldsymbol{u}}} \hat{\mathcal{J}}^{\partial\Omega}\left(\tilde{\boldsymbol{y}},\boldsymbol{u}\right)\mathrm{d}\boldsymbol{x} + \int_{\Omega_{\boldsymbol{u}}} \hat{\mathcal{J}}^{\Omega}\left(\tilde{\boldsymbol{y}},\boldsymbol{u}\right)\mathrm{d}\boldsymbol{x}, \tag{3.3}$$

since this allows us to derive the adjoint also for other applications.

Note, that $\bar{\mathcal{J}}$ acts on $Y(\Omega_{\boldsymbol{u}})\times U$, i.e., on the physical domain. We will also consider its transformation to the reference domain which will be denoted by $\mathcal{J} : Y_{\mathrm{ref}}\times U \to \mathbb{R}$ and will be detailed later. The same holds true for the PDE-system $\bar{\mathcal{R}}$ in (2.6) acting on $Y(\Omega_{\boldsymbol{u}})\times U$ and its analog $\mathcal{R}$ on $Y_{\mathrm{ref}}\times U$. With these preparations at hand, we consider the following constrained optimization problem

$$\bar{\mathcal{J}}(\tilde{\boldsymbol{y}},\boldsymbol{u}) \to \min! \quad \text{s.t.} \quad \bar{\mathcal{R}}(\tilde{\boldsymbol{y}},\boldsymbol{u}) = 0,\ \boldsymbol{u}\in U_{\mathrm{ad}}. \tag{3.4}$$

The mathematical theory of such pde-constraint optimization problems is well-established. As an example, we recall well-known first order optimality conditions.

Lemma 3.1. *Assume that (1) $U_{\mathrm{ad}} \subset U$ is nonempty, convex and closed; (2) $\bar{\mathcal{J}}: Y(\Omega_{\boldsymbol{u}})\times U \to \mathbb{R}$, $\bar{\mathcal{R}}: Y(\Omega_{\boldsymbol{u}})\times U \to Z(\Omega_{\boldsymbol{u}})$ are continuously Fréchet-differentiable;*

(3) The design-to-state operator $\mathcal{S} : U_{\text{ad}} \to Y(\Omega_{\boldsymbol{u}})$, $\mathcal{S}(\boldsymbol{u}) := \tilde{\boldsymbol{y}}(\boldsymbol{u})$ exists in a neighborhood $B(U_{\text{ad}}) \subset U$ of U_{ad} and is continuously Fréchet-differentiable. Then, an optimal solution $(\tilde{\boldsymbol{y}}^*, \boldsymbol{u}^*, \tilde{\boldsymbol{\lambda}}^*) \in Z(\Omega_{\boldsymbol{u}})$ of (3.4) satisfies the following first-order conditions

$$\mathcal{L}_{\tilde{\boldsymbol{\lambda}}}(\tilde{\boldsymbol{y}}^*, \boldsymbol{u}^*, \tilde{\boldsymbol{\lambda}}^*) = \bar{\mathcal{R}}(\tilde{\boldsymbol{y}}^*, \boldsymbol{u}^*)^T = 0,$$
$$\mathcal{L}_{\tilde{\boldsymbol{y}}}(\tilde{\boldsymbol{y}}^*, \boldsymbol{u}^*, \tilde{\boldsymbol{\lambda}}^*) = \bar{\mathcal{J}}_{\tilde{\boldsymbol{y}}}(\tilde{\boldsymbol{y}}^*, \boldsymbol{u}^*) + \langle \tilde{\boldsymbol{\lambda}}^*, \bar{\mathcal{R}}_{\tilde{\boldsymbol{y}}}(\tilde{\boldsymbol{y}}^*, \boldsymbol{u}^*) \rangle_{Z(\Omega_{\boldsymbol{u}})^*, Z(\Omega_{\boldsymbol{u}})} = 0,$$
$$\langle \mathcal{L}_{\boldsymbol{u}}(\tilde{\boldsymbol{y}}^*, \boldsymbol{u}^*, \tilde{\boldsymbol{\lambda}}^*)^T, \boldsymbol{u} - \boldsymbol{u}^* \rangle_{U^*,U} = \langle \bar{\mathcal{J}}_{\boldsymbol{u}}(\tilde{\boldsymbol{y}}^*, \boldsymbol{u}^*)^T + \bar{\mathcal{R}}_{\boldsymbol{u}}(\tilde{\boldsymbol{y}}^*, \boldsymbol{u}^*)^T \tilde{\boldsymbol{\lambda}}^*, \boldsymbol{u} - \boldsymbol{u}^* \rangle_{U^*,U} \geq 0,$$

for all $\boldsymbol{u} \in U_{\text{ad}}$. □

Defining $Z_{\text{ref}} := {Y_{\text{ref}}}^* \times L_2(\Gamma_{\text{ref,in}})$, the general strategy for computing derivatives for our pde-constrained optimization problem can now be described as follows:

1. *Constraint/state equation:* For a given parameter $\boldsymbol{u} \in U_{\text{ad}}$, compute the corresponding state $\tilde{\boldsymbol{y}}(\boldsymbol{u}) \in Y(\Omega_{\boldsymbol{u}})$ by solving the state equation $\bar{\mathcal{R}}(\tilde{\boldsymbol{y}}(\boldsymbol{u}), \boldsymbol{u}) = 0$ in (2.6) on the physical domain $\Omega_{\boldsymbol{u}}$.
2. *Adjoint equation:* Given the state $\tilde{\boldsymbol{y}}(\boldsymbol{u})$, determine the adjoint state $\tilde{\boldsymbol{\lambda}} \in Z(\Omega_{\boldsymbol{u}})^*$ by solving the adjoint equation $\langle \tilde{\boldsymbol{\lambda}}, \bar{\mathcal{R}}_{\tilde{\boldsymbol{y}}}(\tilde{\boldsymbol{y}}(\boldsymbol{u}), \boldsymbol{u})[\widetilde{\delta \boldsymbol{y}}] \rangle_{Z(\Omega_{\boldsymbol{u}})^*, Z(\Omega_{\boldsymbol{u}})} = -\bar{\mathcal{J}}_{\tilde{\boldsymbol{y}}}(\tilde{\boldsymbol{y}}(\boldsymbol{u}), \boldsymbol{u})[\widetilde{\delta \boldsymbol{y}}]$ on the physical domain $\Omega_{\boldsymbol{u}}$ for all $(\tilde{\boldsymbol{y}} + \widetilde{\delta \boldsymbol{y}}) \in Y(\Omega_{\boldsymbol{u}})$.
3. *Reduced derivative:* Evaluate the derivative of the reduced function $j(\boldsymbol{u}) := \mathcal{J}(\boldsymbol{y}(\boldsymbol{u}), \boldsymbol{u})$ with respect to $\boldsymbol{u}$ by $j'(\boldsymbol{u})^T = \nabla_{\boldsymbol{u}} j(\boldsymbol{u}) = \nabla_{\boldsymbol{u}} \mathcal{J}(\boldsymbol{y}(\boldsymbol{u}), \boldsymbol{u}) + \langle \nabla_{\boldsymbol{u}} \mathcal{R}(\boldsymbol{y}(\boldsymbol{u}), \boldsymbol{u}), \boldsymbol{\lambda} \rangle_{Z_{\text{ref}}, {Z_{\text{ref}}}^*}$. Note, that this computation is done on the *reference domain* Ω_{ref}.

The next section is devoted to the detailed derivation of 2. (including the adjoint pde in §3.1 and boundary conditions in §3.2) as well as 3. in §3.3.

3.1. Multiphase Adjoint. We are now going to derive the adjoint system.

3.1.1. Adjoint System for Multiphase Flow. We now detail the adjoint system for the specific case of multiphase incompressible Navier-Stokes flow (2.4) and a *general* objective function $\bar{\mathcal{J}}$ consisting of contributions from the domain $\Omega_{\boldsymbol{u}}$ and the domain boundary $\partial\Omega_{\boldsymbol{u}}$. For the derivation of the adjoint system we consider the change of turbulent quantities due to parameter variations as negligible which is a common approximation called 'frozen turbulence' in literature (cf. [6, 21, 23]).

Proposition 3.2. *For the optimization problem* (3.4) *with $\bar{\mathcal{J}}$ as in* (3.3), *$\bar{\mathcal{R}}$ defined by* (2.6) *and $Y(\Omega_{\boldsymbol{u}})$ as in* (2.5), *the adjoint system amounts finding $\tilde{\boldsymbol{\lambda}} := (\tilde{\boldsymbol{w}}, \tilde{q}, \tilde{\gamma}, \tilde{\gamma}_{\text{in}}) \in Z(\Omega_{\boldsymbol{u}})^*$ such that*

$$-\tilde{\rho} D(\tilde{\boldsymbol{w}})\tilde{\boldsymbol{v}} - \nabla \cdot (\tilde{\mu}_{\mathit{eff}} D(\tilde{\boldsymbol{w}})) - \nabla \tilde{q} - \tilde{\alpha} \nabla \tilde{\gamma} + \hat{\mathcal{J}}^{\Omega}_{\tilde{\boldsymbol{v}}}(\tilde{\boldsymbol{y}}, \boldsymbol{u})^T = 0, \quad \text{on } \Omega_{\boldsymbol{u}}, \tag{3.5a}$$

$$\nabla \cdot \tilde{\boldsymbol{w}} = -\hat{\mathcal{J}}^{\Omega}_{\tilde{p}^*}(\tilde{\boldsymbol{y}}, \boldsymbol{u}), \quad \text{on } \Omega_{\boldsymbol{u}}, \tag{3.5b}$$

$$\begin{aligned}&(\tilde{\mu}_1 - \tilde{\mu}_2)(D(\tilde{\boldsymbol{v}}) : \nabla \tilde{\boldsymbol{w}}) - (\tilde{\rho}_1 - \tilde{\rho}_2)\tilde{\boldsymbol{v}}^T (\nabla \tilde{\boldsymbol{w}})\tilde{\boldsymbol{v}} + \\ &+ (\tilde{\rho}_2 - \tilde{\rho}_1)\boldsymbol{g}^T(\tilde{\boldsymbol{w}} + \tilde{\boldsymbol{x}} \nabla \cdot \tilde{\boldsymbol{w}}) - \tilde{\boldsymbol{v}}^T \nabla \tilde{\gamma} + \hat{\mathcal{J}}^{\Omega}_{\tilde{\alpha}}(\tilde{\boldsymbol{y}}, \boldsymbol{u})^T = 0, \quad \text{on } \Omega_{\boldsymbol{u}}.\end{aligned} \tag{3.5c}$$

$$\begin{aligned}&\int_{\partial\Omega_{\boldsymbol{u}}} \{\widetilde{\delta \boldsymbol{v}}^T \left(\tilde{\rho}\, \tilde{\boldsymbol{n}} \tilde{\boldsymbol{w}}^T \tilde{\boldsymbol{v}} + \tilde{\rho} \tilde{\boldsymbol{w}} \tilde{\boldsymbol{v}}^T \tilde{\boldsymbol{n}} + \tilde{\mu}_{\mathit{eff}} D(\tilde{\boldsymbol{w}})\tilde{\boldsymbol{n}} + \tilde{\boldsymbol{n}}\, \tilde{q} + \tilde{\alpha} \tilde{\gamma}\, \tilde{\boldsymbol{n}}\right) - \\ &- \tilde{\boldsymbol{w}}^T \tilde{\mu}_{\mathit{eff}} D(\widetilde{\delta \boldsymbol{v}})\tilde{\boldsymbol{n}}\} \mathrm{d}S + \bar{\mathcal{J}}^{\partial\Omega}_{\tilde{\boldsymbol{v}}}(\tilde{\boldsymbol{y}}, \boldsymbol{u})[\widetilde{\delta \boldsymbol{v}}] = 0, \quad \text{on } \partial\Omega_{\boldsymbol{u}}\end{aligned} \tag{3.6a}$$

$$\int_{\partial\Omega_{\boldsymbol{u}}} \widetilde{\delta p}\left(\tilde{\boldsymbol{w}}^T\tilde{\boldsymbol{n}}\right)\tilde{\boldsymbol{n}}\mathrm{d}S + \bar{\mathcal{J}}_p^{\partial\Omega}\left(\tilde{\boldsymbol{y}},\boldsymbol{u}\right)[\widetilde{\delta p}] = 0, \qquad \text{on } \partial\Omega_{\boldsymbol{u}}, \tag{3.6b}$$

$$\begin{aligned}&\int_{\partial\Omega_{\boldsymbol{u}}} \widetilde{\delta\alpha}\big(-(\tilde{\mu}_1-\tilde{\mu}_2)\,\tilde{\boldsymbol{w}}^T D(\tilde{\boldsymbol{v}})\tilde{\boldsymbol{n}} + (\tilde{\rho}_1-\tilde{\rho}_2)\,\tilde{\boldsymbol{w}}^T\tilde{\boldsymbol{v}}\tilde{\boldsymbol{v}}^T\tilde{\boldsymbol{n}}+\\ &\quad + (\tilde{\rho}_1-\tilde{\rho}_2)\,\boldsymbol{g}^T\tilde{\boldsymbol{x}}\tilde{\boldsymbol{w}}^T\tilde{\boldsymbol{n}} + \tilde{\gamma}\tilde{\boldsymbol{v}}^T\tilde{\boldsymbol{n}}\Big)\,\mathrm{d}S + \int_{\Gamma_{\boldsymbol{u},\mathrm{in}}}\widetilde{\delta\alpha}\tilde{\gamma}_{\mathrm{in}}\,\mathrm{d}S+\\ &\qquad + \bar{\mathcal{J}}_{\tilde{\alpha}}^{\partial\Omega}\left(\tilde{\boldsymbol{y}},\boldsymbol{u}\right)[\widetilde{\delta\alpha}] = 0, \qquad \text{on } \partial\Omega_{\boldsymbol{u}},\end{aligned} \tag{3.6c}$$

i.e., (3.5) *are the multiphase adjoint Navier-Stokes equations and* (3.6) *are the multiphase adjoint boundary conditions.*

Proof. For the directional derivative of $\bar{\mathcal{R}}\left(\tilde{\boldsymbol{y}}\left(\boldsymbol{u}\right),\boldsymbol{u}\right)$ w.r.t. the flow variables $\tilde{\boldsymbol{y}} = (\tilde{\boldsymbol{v}},\tilde{p}^*,\tilde{\alpha})$ we have $\bar{\mathcal{R}}_{\tilde{\boldsymbol{y}}}\left(\tilde{\boldsymbol{y}}\left(\boldsymbol{u}\right),\boldsymbol{u}\right)[\widetilde{\delta\boldsymbol{y}}] = \bar{\mathcal{R}}_{(\tilde{\boldsymbol{v}},\tilde{p}^*,\tilde{\alpha})}\left((\tilde{\boldsymbol{v}},\tilde{p}^*,\tilde{\alpha}),\boldsymbol{u}\right)[(\widetilde{\delta\boldsymbol{v}},\widetilde{\delta p},\widetilde{\delta\alpha})] = \bar{\mathcal{R}}_{\tilde{\boldsymbol{v}}}\left((\tilde{\boldsymbol{v}},\tilde{p}^*,\tilde{\alpha}),\boldsymbol{u}\right)[\widetilde{\delta\boldsymbol{v}}] + \bar{\mathcal{R}}_{\tilde{p}^*}\left((\tilde{\boldsymbol{v}},\tilde{p}^*,\tilde{\alpha}),\boldsymbol{u}\right)[\widetilde{\delta p}] + \bar{\mathcal{R}}_{\tilde{\alpha}}\left((\tilde{\boldsymbol{v}},\tilde{p}^*,\tilde{\alpha}),\boldsymbol{u}\right)[\widetilde{\delta\alpha}]$. Abbreviating $\bar{\mathcal{R}}_x := \bar{\mathcal{R}}_x\left((\tilde{\boldsymbol{v}},\tilde{p}^*,\tilde{\alpha}),\boldsymbol{u}\right)[\widetilde{\delta x}]$, we get

$$\bar{\mathcal{R}}_{\tilde{\boldsymbol{v}}} = \begin{pmatrix}\nabla\cdot\left(\tilde{\rho}\widetilde{\delta\boldsymbol{v}}\tilde{\boldsymbol{v}}^T\right) + \nabla\cdot\left(\tilde{\rho}\tilde{\boldsymbol{v}}\widetilde{\delta\boldsymbol{v}}^T\right) - \nabla\cdot\left(\tilde{\mu}_{\mathrm{eff}}D(\widetilde{\delta\boldsymbol{v}})\right)\\ \nabla\cdot\widetilde{\delta\boldsymbol{v}}\\ \nabla\cdot\left(\tilde{\alpha}\widetilde{\delta\boldsymbol{v}}\right)\\ 0\end{pmatrix}, \quad \bar{\mathcal{R}}_{\tilde{p}^*} = \begin{pmatrix}\nabla\widetilde{\delta p}\\ 0\\ 0\\ 0\end{pmatrix}$$

and

$$\bar{\mathcal{R}}_{\tilde{\alpha}} = \begin{pmatrix}\nabla\cdot\left(\widetilde{\delta\alpha}\,(\tilde{\rho}_1-\tilde{\rho}_2)\tilde{\boldsymbol{v}}\tilde{\boldsymbol{v}}^T\right) - \nabla\cdot\left(\widetilde{\delta\alpha}\,(\tilde{\mu}_1-\tilde{\mu}_2)D(\tilde{\boldsymbol{v}})\right) + \boldsymbol{g}^T\tilde{\boldsymbol{x}}\nabla\widetilde{\delta\alpha}\,(\tilde{\rho}_1-\tilde{\rho}_2)\\ 0\\ \nabla\cdot\left(\widetilde{\delta\alpha}\tilde{\boldsymbol{v}}\right)\\ \widetilde{\delta\alpha}.\end{pmatrix}.$$

Then, we obtain

$$\begin{aligned}&\langle(\tilde{\boldsymbol{w}},\tilde{q},\tilde{\gamma},\tilde{\gamma}_{\mathrm{in}}),\bar{\mathcal{R}}_{(\tilde{\boldsymbol{v}},\tilde{p}^*,\tilde{\alpha})}\left((\tilde{\boldsymbol{v}},\tilde{p}^*,\tilde{\alpha}),\boldsymbol{u}\right)[(\widetilde{\delta\boldsymbol{v}},\widetilde{\delta p},\widetilde{\delta\alpha})]\rangle_{Z(\Omega_{\boldsymbol{u}})^*,Z(\Omega_{\boldsymbol{u}})} =\\ &= \int_{\Omega_{\boldsymbol{u}}}\tilde{\boldsymbol{w}}^T\nabla\cdot\left(\tilde{\rho}\widetilde{\delta\boldsymbol{v}}\tilde{\boldsymbol{v}}^T\right)\mathrm{d}\tilde{\boldsymbol{x}} + \int_{\Omega_{\boldsymbol{u}}}\tilde{\boldsymbol{w}}^T\nabla\cdot\left(\tilde{\rho}\tilde{\boldsymbol{v}}\widetilde{\delta\boldsymbol{v}}^T\right)\mathrm{d}\tilde{\boldsymbol{x}}\\ &\quad - \int_{\Omega_{\boldsymbol{u}}}\tilde{\boldsymbol{w}}^T\nabla\cdot\left(\tilde{\mu}_{\mathrm{eff}}D(\widetilde{\delta\boldsymbol{v}})\right)\mathrm{d}\tilde{\boldsymbol{x}} + \int_{\Omega_{\boldsymbol{u}}}\tilde{\boldsymbol{w}}^T\nabla\widetilde{\delta p}\,\mathrm{d}\tilde{\boldsymbol{x}}\\ &\quad + \int_{\Omega_{\boldsymbol{u}}}\tilde{\boldsymbol{w}}^T\nabla\cdot\left(\widetilde{\delta\alpha}\,(\tilde{\rho}_1-\tilde{\rho}_2)\tilde{\boldsymbol{v}}\tilde{\boldsymbol{v}}^T\right)\mathrm{d}\tilde{\boldsymbol{x}} - \int_{\Omega_{\boldsymbol{u}}}\tilde{\boldsymbol{w}}^T\nabla\cdot\left(\widetilde{\delta\alpha}\,(\tilde{\mu}_1-\tilde{\mu}_2)D(\nabla\tilde{\boldsymbol{v}})\right)\mathrm{d}\tilde{\boldsymbol{x}}\\ &\quad + \int_{\Omega_{\boldsymbol{u}}}\tilde{\boldsymbol{w}}^T\boldsymbol{g}^T\tilde{\boldsymbol{x}}\nabla\widetilde{\delta\alpha}\,(\tilde{\rho}_1-\tilde{\rho}_2)\mathrm{d}\tilde{\boldsymbol{x}} + \int_{\Omega_{\boldsymbol{u}}}\tilde{q}\nabla\cdot\widetilde{\delta\boldsymbol{v}}\,\mathrm{d}\tilde{\boldsymbol{x}} + \int_{\Omega_{\boldsymbol{u}}}\tilde{\gamma}\nabla\cdot\left(\tilde{\alpha}\widetilde{\delta\boldsymbol{v}}\right)\mathrm{d}\tilde{\boldsymbol{x}}\\ &\quad + \int_{\Omega_{\boldsymbol{u}}}\tilde{\gamma}\nabla\cdot\left(\widetilde{\delta\alpha}\tilde{\boldsymbol{v}}\right)\mathrm{d}\tilde{\boldsymbol{x}} + \int_{\Gamma_{\boldsymbol{u},\mathrm{in}}}\tilde{\gamma}_{\mathrm{in}}\widetilde{\delta\alpha}\,\mathrm{d}S.\end{aligned}$$

Next, we use Gauss' theorem, integration by parts and Green's identity to obtain in a straightforward way

$$\begin{aligned}\int_{\Omega_{\boldsymbol{u}}}\tilde{\boldsymbol{w}}^T\nabla\cdot\left(\tilde{\rho}\widetilde{\delta\boldsymbol{v}}\tilde{\boldsymbol{v}}^T\right)\mathrm{d}\tilde{\boldsymbol{x}} &= -\int_{\Omega_{\boldsymbol{u}}}\nabla\tilde{\boldsymbol{w}} : \left(\tilde{\rho}\widetilde{\delta\boldsymbol{v}}\tilde{\boldsymbol{v}}^T\right)\mathrm{d}\tilde{\boldsymbol{x}} + \int_{\partial\Omega_{\boldsymbol{u}}}\tilde{\boldsymbol{w}}^T\tilde{\rho}\tilde{\boldsymbol{v}}\widetilde{\delta\boldsymbol{v}}^T\tilde{\boldsymbol{n}}\,\mathrm{d}S\\ &= -\int_{\Omega_{\boldsymbol{u}}}\widetilde{\delta\boldsymbol{v}}^T\tilde{\rho}\left(\nabla\tilde{\boldsymbol{w}}\right)\tilde{\boldsymbol{v}}\,\mathrm{d}\tilde{\boldsymbol{x}} + \int_{\partial\Omega_{\boldsymbol{u}}}\widetilde{\delta\boldsymbol{v}}^T\tilde{\rho}\tilde{\boldsymbol{n}}\tilde{\boldsymbol{w}}^T\tilde{\boldsymbol{v}}\,\mathrm{d}S,\end{aligned} \tag{3.7a}$$

(3.7b) $\displaystyle\int_{\Omega_{\boldsymbol{u}}} \tilde{\boldsymbol{w}}^T \nabla\cdot \left(\tilde{\rho}\tilde{\boldsymbol{v}}\widetilde{\delta \boldsymbol{v}}^T\right)\mathrm{d}\tilde{\boldsymbol{x}} = -\int_{\Omega_{\boldsymbol{u}}} \nabla \tilde{\boldsymbol{w}} : \left(\tilde{\rho}\tilde{\boldsymbol{v}}\widetilde{\delta \boldsymbol{v}}^T\right)\mathrm{d}\tilde{\boldsymbol{x}} + \int_{\partial\Omega_{\boldsymbol{u}}} \tilde{\boldsymbol{w}}^T \tilde{\rho}\widetilde{\delta \boldsymbol{v}}\tilde{\boldsymbol{v}}^T \tilde{\boldsymbol{n}}\,\mathrm{d}S$

$\displaystyle = -\int_{\Omega_{\boldsymbol{u}}} \widetilde{\delta \boldsymbol{v}}^T \tilde{\rho}\left(\nabla \tilde{\boldsymbol{w}}\right)^T \tilde{\boldsymbol{v}}\,\mathrm{d}\tilde{\boldsymbol{x}} + \int_{\partial\Omega_{\boldsymbol{u}}} \widetilde{\delta \boldsymbol{v}}^T \tilde{\rho}\tilde{\boldsymbol{w}}\tilde{\boldsymbol{v}}^T \tilde{\boldsymbol{n}}\,\mathrm{d}S,$

(3.7c) $\displaystyle -\int_{\Omega_{\boldsymbol{u}}} \tilde{\boldsymbol{w}}^T \left(\nabla\cdot\left(\tilde{\mu}_{\text{eff}} D(\widetilde{\delta \boldsymbol{v}})\right)\right)\mathrm{d}\tilde{\boldsymbol{x}} = -\int_{\Omega_{\boldsymbol{u}}} \widetilde{\delta \boldsymbol{v}}^T \left(\nabla\cdot\left(\tilde{\mu}_{\text{eff}} D(\tilde{\boldsymbol{w}})\right)\right)\mathrm{d}\tilde{\boldsymbol{x}} +$

$\displaystyle + \int_{\partial\Omega_{\boldsymbol{u}}} \widetilde{\delta \boldsymbol{v}}^T \tilde{\mu}_{\text{eff}} (D(\tilde{\boldsymbol{w}}))\tilde{\boldsymbol{n}}\,\mathrm{d}S - \int_{\partial\Omega_{\boldsymbol{u}}} \tilde{\boldsymbol{w}}^T \tilde{\mu}_{\text{eff}} D(\widetilde{\delta \boldsymbol{v}})\tilde{\boldsymbol{n}}\,\mathrm{d}S,$

(3.7d) $\displaystyle\int_{\Omega_{\boldsymbol{u}}} \tilde{\boldsymbol{w}}^T \nabla\cdot \left(\widetilde{\delta\alpha}\,(\tilde{\rho}_1 - \tilde{\rho}_2)\tilde{\boldsymbol{v}}\tilde{\boldsymbol{v}}^T\right)\mathrm{d}\tilde{\boldsymbol{x}} =$

$\displaystyle = -\int_{\Omega_{\boldsymbol{u}}} \nabla \tilde{\boldsymbol{w}} : \left(\widetilde{\delta\alpha}\,(\tilde{\rho}_1 - \tilde{\rho}_2)\,\tilde{\boldsymbol{v}}\tilde{\boldsymbol{v}}^T\right)\mathrm{d}\tilde{\boldsymbol{x}} + \int_{\partial\Omega_{\boldsymbol{u}}} \tilde{\boldsymbol{w}}^T \widetilde{\delta\alpha}\,(\tilde{\rho}_1 - \tilde{\rho}_2)\,\tilde{\boldsymbol{v}}\tilde{\boldsymbol{v}}^T \tilde{\boldsymbol{n}}\,\mathrm{d}S$

$\displaystyle = -\int_{\Omega_{\boldsymbol{u}}} \widetilde{\delta\alpha}\,(\tilde{\rho}_1 - \tilde{\rho}_2)\,\tilde{\boldsymbol{v}}^T \left(\nabla \tilde{\boldsymbol{w}}\right)^T \tilde{\boldsymbol{v}}\,\mathrm{d}\tilde{\boldsymbol{x}} + \int_{\partial\Omega_{\boldsymbol{u}}} \widetilde{\delta\alpha}\,(\tilde{\rho}_1 - \tilde{\rho}_2)\,\tilde{\boldsymbol{w}}^T \tilde{\boldsymbol{v}}\tilde{\boldsymbol{v}}^T \tilde{\boldsymbol{n}}\,\mathrm{d}S,$

(3.7e) $\displaystyle -\int_{\Omega_{\boldsymbol{u}}} \tilde{\boldsymbol{w}}^T \nabla\cdot \left(\widetilde{\delta\alpha}\,(\tilde{\mu}_1 - \tilde{\mu}_2) D(\tilde{\boldsymbol{v}})\right)\mathrm{d}\tilde{\boldsymbol{x}} =$

$\displaystyle = \int_{\Omega_{\boldsymbol{u}}} \widetilde{\delta\alpha}\,(\tilde{\mu}_1 - \tilde{\mu}_2)\,\nabla \tilde{\boldsymbol{w}} : D(\tilde{\boldsymbol{v}})\,\mathrm{d}\tilde{\boldsymbol{x}} = -\int_{\partial\Omega_{\boldsymbol{u}}} \widetilde{\delta\alpha}\,(\tilde{\mu}_1 - \tilde{\mu}_2)\,\tilde{\boldsymbol{w}}^T D(\tilde{\boldsymbol{v}})\tilde{\boldsymbol{n}}\,\mathrm{d}S,$

(3.7f) $\displaystyle\int_{\Omega_{\boldsymbol{u}}} \tilde{\boldsymbol{w}}^T \boldsymbol{g}^T \tilde{\boldsymbol{x}}\,\nabla\widetilde{\delta\alpha}\,(\tilde{\rho}_1 - \tilde{\rho}_2)\,\mathrm{d}\tilde{\boldsymbol{x}} =$

$\displaystyle = -\int_{\Omega_{\boldsymbol{u}}} \widetilde{\delta\alpha}\,(\tilde{\rho}_1 - \tilde{\rho}_2)\,\nabla\cdot\left(\boldsymbol{g}^T \tilde{\boldsymbol{x}}\,\tilde{\boldsymbol{w}}\right)\mathrm{d}\tilde{\boldsymbol{x}} + \int_{\partial\Omega_{\boldsymbol{u}}} \widetilde{\delta\alpha}\,(\tilde{\rho}_1 - \tilde{\rho}_2)\,\boldsymbol{g}^T \tilde{\boldsymbol{x}}\,\tilde{\boldsymbol{w}}^T \tilde{\boldsymbol{n}}\,\mathrm{d}S$

$\displaystyle = -\int_{\Omega_{\boldsymbol{u}}} \widetilde{\delta\alpha}\,(\tilde{\rho}_1 - \tilde{\rho}_2)\left(\tilde{\boldsymbol{w}}^T \boldsymbol{g} + \boldsymbol{g}^T \tilde{\boldsymbol{x}}\,\nabla\cdot \tilde{\boldsymbol{w}}\right)\mathrm{d}\tilde{\boldsymbol{x}} + \int_{\partial\Omega_{\boldsymbol{u}}} \widetilde{\delta\alpha}\,(\tilde{\rho}_1 - \tilde{\rho}_2)\,\boldsymbol{g}^T \tilde{\boldsymbol{x}}\,\tilde{\boldsymbol{w}}^T \tilde{\boldsymbol{n}}\,\mathrm{d}S,$

(3.7g) $\displaystyle\int_{\Omega_{\boldsymbol{u}}} \tilde{\boldsymbol{w}}^T \nabla\widetilde{\delta p}\,\mathrm{d}\tilde{\boldsymbol{x}} = -\int_{\Omega_{\boldsymbol{u}}} \widetilde{\delta p}\nabla\cdot \tilde{\boldsymbol{w}}\,\mathrm{d}\tilde{\boldsymbol{x}} + \int_{\partial\Omega_{\boldsymbol{u}}} \widetilde{\delta p}\tilde{\boldsymbol{w}}^T \tilde{\boldsymbol{n}}\,\mathrm{d}S,$

(3.7h) $\displaystyle\int_{\Omega_{\boldsymbol{u}}} \tilde{\gamma}\nabla\cdot\left(\tilde{\alpha}\widetilde{\delta \boldsymbol{v}}\right)\mathrm{d}\tilde{\boldsymbol{x}} = -\int_{\Omega_{\boldsymbol{u}}} \widetilde{\delta \boldsymbol{v}}^T \tilde{\alpha}\nabla\tilde{\gamma}\,\mathrm{d}\tilde{\boldsymbol{x}} + \int_{\partial\Omega_{\boldsymbol{u}}} \widetilde{\delta \boldsymbol{v}}^T \tilde{\alpha}\tilde{\gamma}\,\tilde{\boldsymbol{n}}\,\mathrm{d}S,$

(3.7i) $\displaystyle\int_{\Omega_{\boldsymbol{u}}} \tilde{\gamma}\nabla\cdot\left(\widetilde{\delta\alpha}\tilde{\boldsymbol{v}}\right)\mathrm{d}\tilde{\boldsymbol{x}} = \int_{\Omega_{\boldsymbol{u}}} \widetilde{\delta\alpha}\,\tilde{\boldsymbol{v}}^T \nabla\tilde{\gamma}\,\mathrm{d}\tilde{\boldsymbol{x}} + \int_{\partial\Omega_{\boldsymbol{u}}} \widetilde{\delta\alpha}\,\tilde{\gamma}\,\tilde{\boldsymbol{v}}^T \tilde{\boldsymbol{n}}\,\mathrm{d}S.$

Combining (3.7a) - (3.7i) with the objective function we get

$$\bar{\mathcal{J}}_{\tilde{\boldsymbol{y}}}\left(\tilde{\boldsymbol{y}},\boldsymbol{u}\right)[\widetilde{\delta \boldsymbol{y}}] + \langle\tilde{\boldsymbol{\lambda}}, \bar{\mathcal{R}}_{\tilde{\boldsymbol{y}}}\left(\tilde{\boldsymbol{y}},\boldsymbol{u}\right)[\widetilde{\delta \boldsymbol{y}}]\rangle_{Z(\Omega_{\boldsymbol{u}})^*, Z(\Omega_{\boldsymbol{u}})} =$$

$$= \bar{\mathcal{J}}_{(\tilde{\boldsymbol{v}},\tilde{p}^*,\tilde{\alpha})}\left(\left(\tilde{\boldsymbol{v}},\tilde{p}^*,\tilde{\alpha}\right),\boldsymbol{u}\right)[(\widetilde{\delta \boldsymbol{v}},\widetilde{\delta p},\tilde{\alpha})]$$

$$+ \langle\left(\tilde{\boldsymbol{w}},\tilde{q},\tilde{\gamma},\tilde{\gamma}_{\text{in}}\right), \bar{\mathcal{R}}_{(\tilde{\boldsymbol{v}},\tilde{p}^*,\tilde{\alpha})}\left(\left(\tilde{\boldsymbol{v}},\tilde{p}^*,\tilde{\alpha}\right),\boldsymbol{u}\right)[(\widetilde{\delta \boldsymbol{v}},\widetilde{\delta p},\tilde{\alpha})]\rangle_{Z(\Omega_{\boldsymbol{u}})^*, Z(\Omega_{\boldsymbol{u}})}$$

(3.8a) $\displaystyle = \int_{\Omega_{\boldsymbol{u}}} \widetilde{\delta \boldsymbol{v}}^T (-\tilde{\rho} D(\nabla\tilde{\boldsymbol{w}})\tilde{\boldsymbol{v}} - \nabla\cdot\left(\tilde{\mu}_{\text{eff}} D(\nabla\tilde{\boldsymbol{w}})\right) - \nabla\tilde{q} - \tilde{\alpha}\nabla\tilde{\gamma})\,\mathrm{d}\tilde{\boldsymbol{x}} + \mathcal{J}^{\Omega}_{\tilde{\boldsymbol{v}}}\left(\tilde{\boldsymbol{y}},\boldsymbol{u}\right)[\widetilde{\delta \boldsymbol{v}}]$

(3.8b) $\displaystyle + \int_{\Omega_{\boldsymbol{u}}} \widetilde{\delta p}\nabla\cdot \tilde{\boldsymbol{w}}\;\mathrm{d}\tilde{\boldsymbol{x}} + \bar{\mathcal{J}}^{\Omega}_{\tilde{p}^*}\left(\tilde{\boldsymbol{y}},\boldsymbol{u}\right)[\widetilde{\delta p}]$

(3.8c) $\displaystyle + \int_{\Omega_{\boldsymbol{u}}} \widetilde{\delta\alpha}^T \Big((\tilde{\mu}_1 - \tilde{\mu}_2)\left(D(\nabla\tilde{\boldsymbol{v}}) : \nabla\tilde{\boldsymbol{w}}\right) - (\tilde{\rho}_1 - \tilde{\rho}_2)\,\tilde{\boldsymbol{v}}^T \left(\nabla\tilde{\boldsymbol{w}}\right)\tilde{\boldsymbol{v}}$

$\displaystyle - (\tilde{\rho}_1 - \tilde{\rho}_2)\,\boldsymbol{g}^T \left(\tilde{\boldsymbol{w}} + \tilde{\boldsymbol{x}}\nabla\cdot \tilde{\boldsymbol{w}}\right) - \tilde{\boldsymbol{v}}^T \nabla\tilde{\gamma}\Big)\mathrm{d}\tilde{\boldsymbol{x}} + \bar{\mathcal{J}}^{\partial\Omega}_{\tilde{\alpha}}\left(\tilde{\boldsymbol{y}},\boldsymbol{u}\right)[\widetilde{\delta\alpha}]$

$$(3.8d)\quad + \int_{\partial\Omega_{\boldsymbol{u}}} \widetilde{\delta \boldsymbol{v}}^T \Big(\tilde\rho \tilde{\boldsymbol{n}} \tilde{\boldsymbol{w}}^T \tilde{\boldsymbol{v}} + \tilde\rho \tilde{\boldsymbol{w}} \tilde{\boldsymbol{v}}^T \tilde{\boldsymbol{n}} + \tilde\mu_{\text{eff}} D(\nabla \tilde{\boldsymbol{w}}) \tilde{\boldsymbol{n}} + \tilde{\boldsymbol{n}} \tilde q + \tilde\alpha \tilde\gamma \tilde{\boldsymbol{n}}\Big) - \tilde{\boldsymbol{w}}^T \tilde\mu_{\text{eff}} D(\nabla \widetilde{\delta \boldsymbol{v}}) \tilde{\boldsymbol{n}} \, \mathrm{d}S + \bar{\mathcal{J}}^{\partial\Omega}_{\tilde{\boldsymbol{v}}} (\tilde{\boldsymbol{y}}, \boldsymbol{u}) [\widetilde{\delta \boldsymbol{v}}]$$

$$(3.8e)\quad + \int_{\partial\Omega_{\boldsymbol{u}}} \widetilde{\delta p} \left(\tilde{\boldsymbol{w}}^T \tilde{\boldsymbol{n}}\right) \mathrm{d}S + \bar{\mathcal{J}}^{\partial\Omega}_{\tilde p^*} (\tilde{\boldsymbol{y}}, \boldsymbol{u}) [\widetilde{\delta p}]$$

$$(3.8f)\quad + \int_{\partial\Omega_{\boldsymbol{u}}} \widetilde{\delta\alpha} \Big(- (\tilde\mu_1 - \tilde\mu_2)\, \tilde{\boldsymbol{w}}^T D(\nabla \tilde{\boldsymbol{v}}) \tilde{\boldsymbol{n}} + (\tilde\rho_1 - \tilde\rho_2)\, \tilde{\boldsymbol{w}}^T \tilde{\boldsymbol{v}} \tilde{\boldsymbol{v}}^T \tilde{\boldsymbol{n}} + (\tilde\rho_1 - \tilde\rho_2)\, \boldsymbol{g}^T \tilde{\boldsymbol{x}} \tilde{\boldsymbol{w}}^T \tilde{\boldsymbol{n}} + \tilde\gamma \tilde{\boldsymbol{v}}^T \tilde{\boldsymbol{n}}\Big) \mathrm{d}S + \int_{\Gamma_{\boldsymbol{u},\text{in}}} \widetilde{\delta\alpha} \tilde\gamma_{\text{in}} \, \mathrm{d}S + \bar{\mathcal{J}}^{\partial\Omega}_{\tilde\alpha} (\tilde{\boldsymbol{y}}, \boldsymbol{u}) [\widetilde{\delta\alpha}]$$

$$= 0.$$

This needs to hold for all $(\tilde{\boldsymbol{v}} + \widetilde{\delta \boldsymbol{v}}, \tilde p^* + \widetilde{\delta p}, \tilde\alpha + \widetilde{\delta\alpha}) \in Y(\Omega_{\boldsymbol{u}})$. Hence, the terms (3.8a)-(3.8f) have to vanish individually, which yields (3.5),(3.6). ☐

REMARK 3.3. *For the terms arising from the differentiation of the convection terms in the momentum and phase fraction equations we could also apply a different treatment than the application of Gauss' theorem in* (3.7a) *and integration by parts in* (3.7h)*. Alternatively, we could just dissolve the divergence and cancel the terms containing $\nabla \cdot \delta \boldsymbol{v}$ due to the continuity equation. With this modification we no longer get boundary contributions from those terms and in the adjoint equations the term $-\tilde\rho\, (\nabla \tilde{\boldsymbol{w}})\, \tilde{\boldsymbol{v}}$ is replaced by $\tilde\rho\, (\nabla \tilde{\boldsymbol{v}})\, \tilde{\boldsymbol{w}} + \tilde{\boldsymbol{w}}^T \tilde{\boldsymbol{v}} \nabla \tilde\rho$ and the term $-\tilde\alpha \nabla \tilde\gamma$ is replaced by $\tilde\gamma \nabla \tilde\alpha$. This alternative treatment for convection terms is pursued for instance by [1, 4, 12, 28], the treatment presented first is utilized e.g. in [17, 21, 26].* ☐

3.2. Adjoint boundary conditions for rigid body motions. Now, we are going to detail the adjoint system (3.5), (3.6) for the specific case of the rigid body motion, i.e., with the function $\bar{\mathcal{J}}_{\text{RBM}}$ defined in (3.1). First, this implies that $\mathcal{J}^\Omega = 0$, so that (3.5) reads

$$(3.9a)\quad -\tilde\rho D(\tilde{\boldsymbol{w}}) \tilde{\boldsymbol{v}} - \nabla \cdot (\tilde\mu_{\text{eff}} D(\tilde{\boldsymbol{w}})) - \nabla \tilde q - \tilde\alpha \nabla \tilde\gamma = 0, \quad \text{on } \Omega_{\boldsymbol{u}},$$

$$(3.9b)\quad \nabla \cdot \tilde{\boldsymbol{w}} = 0, \quad \text{on } \Omega_{\boldsymbol{u}},$$

$$(3.9c)\quad (\tilde\mu_1 - \tilde\mu_2)\, (D(\tilde{\boldsymbol{v}}) : \nabla \tilde{\boldsymbol{w}}) - (\tilde\rho_1 - \tilde\rho_2)\, \tilde{\boldsymbol{v}}^T \left(\nabla \tilde{\boldsymbol{w}}\right) \tilde{\boldsymbol{v}} + {} + (\tilde\rho_2 - \tilde\rho_1)\, \boldsymbol{g}^T \left(\tilde{\boldsymbol{w}} + \tilde{\boldsymbol{x}} \nabla \cdot \tilde{\boldsymbol{w}}\right) - \tilde{\boldsymbol{v}}^T \nabla \tilde\gamma = 0, \quad \text{on } \Omega_{\boldsymbol{u}}.$$

In particular, (3.9b) then implies that $\tilde{\boldsymbol{w}}$ is divergence-free, which will frequently be used in the sequel. Moreover, as $\tilde{\boldsymbol{y}} = (\tilde{\boldsymbol{v}}, \tilde p^*, \tilde\alpha) \in Y(\Omega_{\boldsymbol{u}})$ we have that $\nabla \cdot \tilde{\boldsymbol{v}} = 0$, and equally $\widetilde{\delta \boldsymbol{v}}$ is divergence-free if $(\tilde{\boldsymbol{v}} + \widetilde{\delta \boldsymbol{v}}, \tilde p^* + \widetilde{\delta p^*}, \tilde\alpha + \widetilde{\delta\alpha}) \in Y(\Omega_{\boldsymbol{u}})$.

The boundary conditions in (3.6) so far do not have an appropriate form as the perturbations $\widetilde{\delta \boldsymbol{v}}$, $\widetilde{\delta p}$ and $\widetilde{\delta\alpha}$ still appear. Thus, we detail these conditions. Recall the relevant boundary conditions for the primal multiphase system in (2.4d)-(2.4f). In a first step, we use standard tools (mainly the product rule) in order to simplify the first multiphase adjoint boundary condition in (3.6a).

LEMMA 3.4. *Let $\widetilde{\delta \boldsymbol{v}}$ and $\tilde{\boldsymbol{w}}$ be sufficiently smooth divergence-free vector fields. With $\tilde z_n := \tilde{\boldsymbol{z}}^T \tilde{\boldsymbol{n}}$ as the coefficient of the normal component of some $\tilde{\boldsymbol{z}}$, we have*

$$(3.10)\quad \int_{\partial\Omega_{\boldsymbol{u}}} \left(\widetilde{\delta \boldsymbol{v}}^T \tilde\mu_{\textit{eff}} \nabla \tilde{\boldsymbol{w}} - \tilde{\boldsymbol{w}}^T \mu_{\textit{eff}} \nabla \widetilde{\delta \boldsymbol{v}}\right) \tilde{\boldsymbol{n}} \, \mathrm{d}S = - \int_{\partial\Omega_{\boldsymbol{u}}} \nabla \tilde\mu_{\textit{eff}}^T \left(\tilde w_n \widetilde{\delta \boldsymbol{v}} - \widetilde{\delta v_n} \tilde{\boldsymbol{w}}\right) \mathrm{d}S.$$

Proof. We start by applying the usual product rule to $\nabla(\tilde{\mu}_{\text{eff}}\tilde{\boldsymbol{w}})$ and obtain

$$\int_{\partial\Omega_{\boldsymbol{u}}} \widetilde{\delta\boldsymbol{v}}^T \tilde{\mu}_{\text{eff}} (\nabla\tilde{\boldsymbol{w}})\, \tilde{\boldsymbol{n}}\, \mathrm{d}S = \int_{\partial\Omega_{\boldsymbol{u}}} \widetilde{\delta\boldsymbol{v}}^T \nabla(\tilde{\mu}_{\text{eff}}\tilde{\boldsymbol{w}})\, \tilde{\boldsymbol{n}}\, \mathrm{d}S - \int_{\partial\Omega_{\boldsymbol{u}}} \widetilde{\delta\boldsymbol{v}}^T \nabla\tilde{\mu}_{\text{eff}}\tilde{\boldsymbol{w}}^T\tilde{\boldsymbol{n}}\, \mathrm{d}S.$$

Next, we apply Green's first identity twice and get:

$$\begin{aligned}
\int_{\partial\Omega_{\boldsymbol{u}}} \widetilde{\delta\boldsymbol{v}}^T \nabla(\tilde{\mu}_{\text{eff}}\tilde{\boldsymbol{w}})\, \tilde{\boldsymbol{n}}\, \mathrm{d}S &= \int_{\Omega_{\boldsymbol{u}}} \nabla\widetilde{\delta\boldsymbol{v}}^T : \nabla(\tilde{\mu}_{\text{eff}}\tilde{\boldsymbol{w}})\, \mathrm{d}\tilde{\boldsymbol{x}} + \int_{\Omega_{\boldsymbol{u}}} \widetilde{\delta\boldsymbol{v}}^T \left(\nabla\cdot\left(\nabla(\tilde{\mu}_{\text{eff}}\tilde{\boldsymbol{w}})^T\right)\right) \mathrm{d}\tilde{\boldsymbol{x}} \\
&= \int_{\Omega_{\boldsymbol{u}}} \nabla(\tilde{\mu}_{\text{eff}}\tilde{\boldsymbol{w}})^T : \nabla\widetilde{\delta\boldsymbol{v}}\, \mathrm{d}\tilde{\boldsymbol{x}} + \int_{\Omega_{\boldsymbol{u}}} \widetilde{\delta\boldsymbol{v}}^T \left(\nabla\cdot\left(\nabla(\tilde{\mu}_{\text{eff}}\tilde{\boldsymbol{w}})^T\right)\right) \mathrm{d}\tilde{\boldsymbol{x}} \\
&= \int_{\partial\Omega_{\boldsymbol{u}}} \tilde{\mu}_{\text{eff}}\tilde{\boldsymbol{w}}^T \left(\nabla\widetilde{\delta\boldsymbol{v}}\right)\tilde{\boldsymbol{n}}\, \mathrm{d}S - \int_{\Omega_{\boldsymbol{u}}} \{\tilde{\mu}_{\text{eff}}\tilde{\boldsymbol{w}}^T \underbrace{(\nabla\cdot(\nabla\widetilde{\delta\boldsymbol{v}}^T))}_{=\nabla(\nabla\cdot\widetilde{\delta\boldsymbol{v}})=0} + \widetilde{\delta\boldsymbol{v}}^T (\nabla\cdot(\nabla(\tilde{\mu}_{\text{eff}}\tilde{\boldsymbol{w}})^T))\}\mathrm{d}\tilde{\boldsymbol{x}}.
\end{aligned}$$

For the remaining term we apply the relation $\nabla\cdot(\nabla(\tilde{\mu}_{\text{eff}}\tilde{\boldsymbol{w}})^T) = \nabla(\nabla\cdot(\tilde{\mu}_{\text{eff}}\tilde{\boldsymbol{w}})) = \nabla(\tilde{\boldsymbol{w}}^T\nabla\tilde{\mu}_{\text{eff}}) + \nabla(\tilde{\mu}_{\text{eff}}(\nabla\cdot\tilde{\boldsymbol{w}}))$, where the last term vanishes since $\nabla\cdot\tilde{\boldsymbol{w}} = 0$. Then, integration by parts yields

$$\int_{\Omega_{\boldsymbol{u}}} \widetilde{\delta\boldsymbol{v}}^T \left(\nabla\left(\tilde{\boldsymbol{w}}^T\nabla\tilde{\mu}_{\text{eff}}\right)\right) \mathrm{d}\tilde{\boldsymbol{x}} = -\int_{\Omega_{\boldsymbol{u}}} \nabla\tilde{\mu}_{\text{eff}}^T\tilde{\boldsymbol{w}} \underbrace{\left(\nabla\cdot\widetilde{\delta\boldsymbol{v}}\right)}_{=0} \mathrm{d}\tilde{\boldsymbol{x}} - \int_{\partial\Omega_{\boldsymbol{u}}} \nabla\tilde{\mu}_{\text{eff}}^T\tilde{\boldsymbol{w}}\widetilde{\delta\boldsymbol{v}}^T\tilde{\boldsymbol{n}}\, \mathrm{d}S,$$

which leads to

$$\begin{aligned}
\int_{\partial\Omega_{\boldsymbol{u}}} \widetilde{\delta\boldsymbol{v}}^T \tilde{\mu}_{\text{eff}}(\nabla\tilde{\boldsymbol{w}})\tilde{\boldsymbol{n}}\, dS &= \int_{\partial\Omega_{\boldsymbol{u}}} \widetilde{\delta\boldsymbol{v}}^T \nabla(\tilde{\mu}_{\text{eff}}\tilde{\boldsymbol{w}})\tilde{\boldsymbol{n}}\, dS - \int_{\partial\Omega_{\boldsymbol{u}}} \widetilde{\delta\boldsymbol{v}}^T \nabla\tilde{\mu}_{\text{eff}}\, \tilde{\boldsymbol{w}}^T\tilde{\boldsymbol{n}}\, dS \\
&= \int_{\partial\Omega_{\boldsymbol{u}}} \tilde{\mu}_{\text{eff}}\tilde{\boldsymbol{w}}^T(\nabla\widetilde{\delta\boldsymbol{v}})\tilde{\boldsymbol{n}} dS - \int_{\Omega_{\boldsymbol{u}}} \widetilde{\delta\boldsymbol{v}}^T(\nabla\cdot(\nabla\tilde{\mu}_{\text{eff}}\, \tilde{\boldsymbol{w}})^T))d\boldsymbol{x} - \int_{\partial\Omega_{\boldsymbol{u}}} \widetilde{\delta\boldsymbol{v}}^T \nabla\tilde{\mu}_{\text{eff}}\, \tilde{\boldsymbol{w}}_n\, dS \\
&= \int_{\partial\Omega_{\boldsymbol{u}}} \tilde{\mu}_{\text{eff}}\, \tilde{\boldsymbol{w}}^T(\nabla\widetilde{\delta\boldsymbol{v}})\, \tilde{\boldsymbol{n}}\, dS - \int_{\Omega_{\boldsymbol{u}}} \widetilde{\delta\boldsymbol{v}}^T(\nabla(\tilde{\boldsymbol{w}}^T\, \nabla\tilde{\mu}_{\text{eff}}))d\boldsymbol{x} - \int_{\partial\Omega_{\boldsymbol{u}}} \widetilde{\delta\boldsymbol{v}}^T \nabla\tilde{\mu}_{\text{eff}}\, \tilde{\boldsymbol{w}}_n\, dS \\
&= \int_{\partial\Omega_{\boldsymbol{u}}} \tilde{\mu}_{\text{eff}}\, \tilde{\boldsymbol{w}}^T(\nabla\widetilde{\delta\boldsymbol{v}})\, \tilde{\boldsymbol{n}}\, dS + \int_{\partial\Omega_{\boldsymbol{u}}} \nabla\tilde{\mu}_{\text{eff}}^T\tilde{\boldsymbol{w}}\, \widetilde{\delta\boldsymbol{v}}^T\, \tilde{\boldsymbol{n}}\, dS - \int_{\partial\Omega_{\boldsymbol{u}}} \widetilde{\delta\boldsymbol{v}}^T \nabla\tilde{\mu}_{\text{eff}}\, \tilde{\boldsymbol{w}}_n\, dS \\
&= \int_{\partial\Omega_{\boldsymbol{u}}} \tilde{\boldsymbol{w}}^T\, \tilde{\mu}_{\text{eff}}\, \nabla\widetilde{\delta\boldsymbol{v}}\, \tilde{\boldsymbol{n}}\, dS - \int_{\partial\Omega_{\boldsymbol{u}}} \nabla\tilde{\mu}_{\text{eff}}^T\, (\tilde{\boldsymbol{w}}_n\widetilde{\delta\boldsymbol{v}} - \widetilde{\delta v_n}\tilde{\boldsymbol{w}})dS,
\end{aligned}$$

which proves the claim. □

As already pointed out earlier, the assumption of Lemma 3.4 is fulfilled for rigid body motions so that we can further simplify the first multiphase adjoint boundary condition (3.6a) for the rigid body motion as follows

$$\begin{aligned}
\text{(3.6a')} \quad \int_{\partial\Omega_{\boldsymbol{u}}} \{\widetilde{\delta\boldsymbol{v}}^T\big(\tilde{\rho}\,\tilde{\boldsymbol{n}}\tilde{\boldsymbol{w}}^T\tilde{\boldsymbol{v}} + \tilde{\rho}\tilde{\boldsymbol{w}}\tilde{\boldsymbol{v}}^T\tilde{\boldsymbol{n}} + \tilde{\mu}_{\text{eff}}(\nabla\tilde{\boldsymbol{w}})^T\tilde{\boldsymbol{n}} + \tilde{\boldsymbol{n}}\,\tilde{q} + \tilde{\alpha}\tilde{\gamma}\,\tilde{\boldsymbol{n}}\big) - \tilde{\boldsymbol{w}}^T\tilde{\mu}_{\text{eff}}(\nabla(\widetilde{\delta\boldsymbol{v}}))^T\tilde{\boldsymbol{n}} \\
-\nabla\tilde{\mu}_{\text{eff}}^T\big(\tilde{w}_n\widetilde{\delta\boldsymbol{v}} - \widetilde{\delta v_n}\tilde{\boldsymbol{w}}\big)\}\mathrm{d}S + \bar{\mathcal{J}}_{\tilde{\boldsymbol{v}}}^{\partial\Omega}(\tilde{\boldsymbol{y}},\boldsymbol{u})\,[\widetilde{\delta\boldsymbol{v}}] = 0,
\end{aligned}$$

Recall that $\bar{\mathcal{J}}^{\partial\Omega}(\tilde{\boldsymbol{y}},\boldsymbol{u}) = \int_{\Gamma_{\boldsymbol{u},\text{B}}} \hat{\mathcal{J}}^{\partial\Omega}(\tilde{\boldsymbol{y}},\boldsymbol{u})\, d\boldsymbol{x}$, which means that

$$\hat{\mathcal{J}}^{\partial\Omega}(\tilde{\boldsymbol{y}},\boldsymbol{u}) = 0 \qquad \text{on} \qquad \Gamma_{\boldsymbol{u}} \setminus \Gamma_{\boldsymbol{u},\text{B}} = \Gamma_{\boldsymbol{u},\text{in}} \cup \Gamma_{\boldsymbol{u},\text{out}} \cup \Gamma_{\boldsymbol{u},\text{wall}}.$$

We will now consider the different parts of the boundary individually.

3.2.1. Inlet Boundaries. We start by investigating the inlet boundaries $\Gamma_{\boldsymbol{u},\text{in}}$. As usual we assume that the inlet boundary is sufficiently far from the object so that reflections do not occur, i.e., we obtain $\tilde{\boldsymbol{n}}^T \nabla \widetilde{\delta \boldsymbol{v}}_t = 0$. Since $\tilde{\boldsymbol{y}} + \widetilde{\delta \boldsymbol{y}} \in Y(\Omega_{\boldsymbol{u}})$, we get $\nabla \cdot (\widetilde{\delta \boldsymbol{v}}) = 0$ and $\widetilde{\delta \boldsymbol{v}}_{|\Gamma_{\boldsymbol{u},\text{in}}} = 0$. Hence, the boundary condition in (3.6a') reads

$$\int_{\partial\Omega_{\boldsymbol{u}}} \tilde{\boldsymbol{w}}^T \tilde{\mu}_{\text{eff}} (\nabla(\widetilde{\delta \boldsymbol{v}}))^T \tilde{\boldsymbol{n}}\, dS = 0. \tag{3.6a"}$$

We will first show that the following condition is always satisfied. For any vector $\boldsymbol{z}$ and a normal vector $\boldsymbol{n}$, we define its normal components as $\boldsymbol{z}_n := z_n\, \boldsymbol{n} = (\boldsymbol{z}^T \boldsymbol{n})\, \boldsymbol{n}$ and its tangential component as $\boldsymbol{z}_t := \boldsymbol{z} \times \boldsymbol{n}$. The following relations are then well-known

$$\nabla \cdot \boldsymbol{z}_t = \boldsymbol{n}^T (\nabla \times \boldsymbol{z}) - \boldsymbol{z}^T (\nabla \times \boldsymbol{n}), \qquad \nabla \cdot \boldsymbol{z}_n = (\nabla(\boldsymbol{z}^T \boldsymbol{n}))^T \boldsymbol{n} + (\boldsymbol{z}^T \boldsymbol{n})\, \nabla \cdot \boldsymbol{n}.$$

Applying this to $\boldsymbol{z} = \widetilde{\delta \boldsymbol{v}}$ and recalling that $\nabla \cdot (\widetilde{\delta \boldsymbol{v}}) = 0$ as well as $\widetilde{\delta \boldsymbol{v}}_{|\Gamma_{\boldsymbol{u},\text{in}}} = 0$ yields $\nabla \cdot (\widetilde{\delta \boldsymbol{v}_t}) = 0$ and thus $0 = \nabla \cdot \widetilde{\delta \boldsymbol{v}} = (\nabla(\widetilde{\delta \boldsymbol{v}_n}))^T \tilde{\boldsymbol{n}}$, so that $\nabla(\widetilde{\delta \boldsymbol{v}})^T \tilde{\boldsymbol{n}} = (\nabla(\widetilde{\delta \boldsymbol{v}_n}))^T \tilde{\boldsymbol{n}} + (\nabla(\widetilde{\delta \boldsymbol{v}_t}))^T = (\nabla(\widetilde{\delta \boldsymbol{v}_t}))^T$, which vanishes since we assumed that $\Gamma_{\boldsymbol{u},\text{in}}$ is sufficiently far from $\Gamma_{\boldsymbol{u},\text{B}}$. Hence (3.6a") holds.

Next, we consider (3.6b), which reads here $\int_{\Gamma_{\boldsymbol{u},\text{in}}} \widetilde{\delta p}\, \boldsymbol{w}_n\, dS = 0$ for all $\widetilde{\delta p}$, i.e., $\boldsymbol{w}_n = 0$ on $\Gamma_{\boldsymbol{u},\text{in}}$. Finally, we insert the primal boundary conditions (2.4f, 2.4g) into (3.6c) to obtain (recall $\tilde{\boldsymbol{w}}^T \tilde{\boldsymbol{n}} = 0$ as well as $\bar{\mathcal{J}}^{\partial\Omega}(\cdot, \boldsymbol{u}) = 0$ on $\Gamma_{\boldsymbol{u},\text{in}}$)

$$\begin{aligned}
\int_{\Gamma_{\boldsymbol{u},\text{in}}} \widetilde{\delta\alpha}\, \tilde{\gamma}_{\text{in}}\, \mathrm{d}S = \int_{\Gamma_{\boldsymbol{u},\text{in}}} \widetilde{\delta\alpha} \Big(&(\tilde{\mu}_1 - \tilde{\mu}_2)\, \tilde{\boldsymbol{w}}^T D(\tilde{\boldsymbol{v}}) \tilde{\boldsymbol{n}} - (\tilde{\rho}_1 - \tilde{\rho}_2)\, \tilde{\boldsymbol{w}}^T \tilde{\boldsymbol{v}} \tilde{\boldsymbol{v}}^T \tilde{\boldsymbol{n}} \\
&- (\tilde{\rho}_1 - \tilde{\rho}_2)\, \boldsymbol{g}^T \tilde{\boldsymbol{x}} \tilde{\boldsymbol{w}}^T \tilde{\boldsymbol{n}} - \tilde{\gamma} \tilde{\boldsymbol{v}}^T \tilde{\boldsymbol{n}} \Big)\, \mathrm{d}S \\
= \int_{\Gamma_{\boldsymbol{u},\text{in}}} \widetilde{\delta\alpha} \Big(&(\tilde{\mu}_1 - \tilde{\mu}_2)\, \tilde{\boldsymbol{w}}^T D(\tilde{\boldsymbol{v}}_{\text{in}}) \tilde{\boldsymbol{n}} - (\tilde{\rho}_1 - \tilde{\rho}_2)\, \tilde{\boldsymbol{w}}^T \tilde{\boldsymbol{v}}_{\text{in}} \tilde{\boldsymbol{v}}_{\text{in}}^T \tilde{\boldsymbol{n}} - \tilde{\gamma} \tilde{\boldsymbol{v}}_{\text{in}}^T \tilde{\boldsymbol{n}} \Big)\, \mathrm{d}S.
\end{aligned}$$

Since this needs to hold for all $\widetilde{\delta\alpha}$, we get the condition

$$\tilde{\gamma}_{\text{in}} = (\tilde{\mu}_1 - \tilde{\mu}_2)\, \tilde{\boldsymbol{w}}^T D(\nabla \tilde{\boldsymbol{v}}_{\text{in}}) \tilde{\boldsymbol{n}} - (\tilde{\rho}_1 - \tilde{\rho}_2)\, \tilde{\boldsymbol{w}}^T \tilde{\boldsymbol{v}}_{\text{in}} \tilde{\boldsymbol{v}}_{\text{in}}^T \tilde{\boldsymbol{n}} - \tilde{\gamma} \tilde{\boldsymbol{v}}_{\text{in}}^T \tilde{\boldsymbol{n}}, \qquad \text{on } \Gamma_{\boldsymbol{u},\text{in}}.$$

Note, that we obtain no conditions for the tangential part of the velocity $\tilde{\boldsymbol{w}}_t$, the adjoint pressure $\tilde{q}$ and the adjoint phase fraction $\tilde{\gamma}$. Therefore, we choose homogeneous Neumann conditions for those variables in order to ensure well-posedness:

$$(\tilde{\boldsymbol{n}} \cdot \nabla)\, \tilde{\boldsymbol{w}}_t = 0, \quad \nabla \tilde{q}^T \tilde{\boldsymbol{n}} = 0, \quad \nabla \tilde{\gamma}^T \tilde{\boldsymbol{n}} = 0, \qquad \text{on } \Gamma_{\boldsymbol{u},\text{in}}.$$

3.2.2. Wall boundaries. Next, we consider the boundary part $\Gamma_{\boldsymbol{u},\text{wall}}$, where $\bar{\mathcal{J}}_{\text{RBM}}$ also vanishes. As above for the inlet boundary, we have that $\nabla \cdot (\widetilde{\delta \boldsymbol{v}}) = 0$ and due to the no-slip boundary conditions on $\Gamma_{\boldsymbol{u},\text{wall}}$ we get $\widetilde{\delta \boldsymbol{v}}_{|\Gamma_{\boldsymbol{u},\text{wall}}} = 0$. Hence (3.6a) reduces to

$$0 = \int_{\Gamma_{\boldsymbol{u},\text{wall}}} \tilde{\mu}_{\text{eff}}\, \tilde{\boldsymbol{w}}^T D(\widetilde{\delta \boldsymbol{v}})\, \tilde{\boldsymbol{n}}\, dS = \int_{\Gamma_{\boldsymbol{u},\text{wall}}} \tilde{\mu}_{\text{eff}}\, \tilde{\boldsymbol{w}}^T \nabla(\widetilde{\delta \boldsymbol{v}_t})^T\, \tilde{\boldsymbol{n}}\, dS, \tag{3.11}$$

where the last step is exactly as in §3.2.1 above. For arbitrary vectors $\boldsymbol{w}$ and $\boldsymbol{z}$, the following relation is also well-known

$$\begin{aligned}
\boldsymbol{w}_n^T (\nabla \boldsymbol{z}_t)^T \boldsymbol{n} &= (\boldsymbol{w}^T \boldsymbol{n})\, \boldsymbol{n}^T\, (\nabla(\boldsymbol{z} \times \boldsymbol{n}))^T \boldsymbol{n} = (\boldsymbol{w}^T \boldsymbol{n})\, \boldsymbol{n}^T\, ((\nabla \boldsymbol{z}) \times \boldsymbol{n} + \boldsymbol{z} \times (\nabla \boldsymbol{n}))^T \boldsymbol{n} \\
&= (\boldsymbol{w}^T \boldsymbol{n})\, \boldsymbol{n}^T (\boldsymbol{z} \times (\nabla \boldsymbol{n}))^T \boldsymbol{n} = 0
\end{aligned}$$

due to orthogonality of tangential and normal vectors. Applying this for $\boldsymbol{z} = \widetilde{\delta \boldsymbol{v}}$ yields $\tilde{\boldsymbol{w}}_n^T (\nabla \widetilde{\delta \boldsymbol{v}}_t)^T \tilde{\boldsymbol{n}} = 0$ since $\widetilde{\delta \boldsymbol{v}}_{|\Gamma_{\boldsymbol{u},\mathrm{wall}}} = 0$. By splitting $\tilde{\boldsymbol{w}} = \tilde{\boldsymbol{w}}_t + \tilde{\boldsymbol{w}}_n$, (3.11) now reads

$$0 = \int_{\Gamma_{\boldsymbol{u},\mathrm{wall}}} \tilde{\mu}_{\mathrm{eff}}\, \tilde{\boldsymbol{w}}_t^T\, \nabla(\widetilde{\delta \boldsymbol{v}_t})^T\, \tilde{\boldsymbol{n}}\, dS. \tag{3.12}$$

From the well-known boundary layer theory (see e.g. [24]) it is known that on no-slip wall boundaries we have $\nabla \tilde{\boldsymbol{v}}_t^T\, \tilde{\boldsymbol{n}} \neq 0$ and thus $\nabla(\widetilde{\delta \boldsymbol{v}_t})^T \tilde{\boldsymbol{n}} \neq 0$, so that (3.12) implies that $\tilde{\boldsymbol{w}}_t = 0$ on $\Gamma_{\boldsymbol{u},\mathrm{wall}}$. Next, we obtain by (3.6b) as in §3.2.1 that $\tilde{\boldsymbol{w}}_n = 0$ also on $\Gamma_{\boldsymbol{u},\mathrm{wall}}$, so that $\tilde{\boldsymbol{w}}_{|\Gamma_{\boldsymbol{u},\mathrm{wall}}} = 0$.

Finally, inserting the homogeneous boundary condition on $\tilde{\boldsymbol{w}}$ into (3.6c) results in $0 = \int_{\Gamma_{\boldsymbol{u},\mathrm{wall}}} \widetilde{\delta\alpha}\, \tilde{\gamma}\, \tilde{\boldsymbol{v}}^T\, \tilde{\boldsymbol{n}}\, dS$ for all $\widetilde{\delta\alpha}$. In view of the primal boundary conditions (2.4d), i.e., $\tilde{\boldsymbol{v}}_{|\Gamma_{\boldsymbol{u},\mathrm{wall}}} = 0$, the latter condition is automatically satisfied so that we do not get any further requirements for $\tilde{q}$ and $\tilde{\gamma}$. Consequently, we choose Neumann boundary conditions on $\Gamma_{\boldsymbol{u},\mathrm{wall}}$ for these variables, i.e.,

$$\nabla \tilde{q}^T \tilde{\boldsymbol{n}} = 0, \quad \nabla \tilde{\gamma}^T \tilde{\boldsymbol{n}} = 0 \qquad \text{on } \Gamma_{\boldsymbol{u},\mathrm{wall}}.$$

3.2.3. Body boundary conditions. Next, we consider $\Gamma_{\boldsymbol{u},\mathrm{B}}$, i.e., the boundary of the rigid body. Using Lemma 3.4, $\widetilde{\delta \boldsymbol{v}} = 0$ and recalling that $\bar{\mathcal{J}}^{\partial\Omega}(\tilde{\boldsymbol{y}}, \boldsymbol{u}) \neq 0$, the remaining boundary conditions of (3.6) on $\Gamma_{\boldsymbol{u},\mathrm{B}}$ are:

$$-\int_{\Gamma_{\boldsymbol{u},\mathrm{B}}} \tilde{\boldsymbol{w}}^T \tilde{\mu}_{\mathrm{eff}} \nabla \widetilde{\delta \boldsymbol{v}}^T\, \tilde{\boldsymbol{n}}\, \mathrm{d}S = -\bar{\mathcal{J}}^{\partial\Omega}_{\tilde{\boldsymbol{v}}}(\tilde{\boldsymbol{y}}, \boldsymbol{u})\, [\widetilde{\delta \boldsymbol{v}}], \tag{3.13a}$$

$$\int_{\Gamma_{\boldsymbol{u},\mathrm{B}}} \widetilde{\delta p}\, \left(\tilde{\boldsymbol{w}}^T \tilde{\boldsymbol{n}}\right) \mathrm{d}S = -\bar{\mathcal{J}}^{\partial\Omega}_{p}(\tilde{\boldsymbol{y}}, \boldsymbol{u})\, [\widetilde{\delta p}], \tag{3.13b}$$

$$\int_{\Gamma_{\boldsymbol{u},\mathrm{B}}} \widetilde{\delta\alpha}\big((\tilde{\mu}_2 - \tilde{\mu}_1)\tilde{\boldsymbol{w}}^T D(\tilde{\boldsymbol{v}})\tilde{\boldsymbol{n}} + (\tilde{\rho}_1 - \tilde{\rho}_2)\boldsymbol{g}^T \tilde{\boldsymbol{x}} \tilde{\boldsymbol{w}}^T \tilde{\boldsymbol{n}}\big)\, \mathrm{d}S = -\bar{\mathcal{J}}^{\partial\Omega}_{\tilde{\alpha}}(\tilde{\boldsymbol{y}}, \boldsymbol{u})[\widetilde{\delta\alpha}]. \tag{3.13c}$$

As opposed to the previous cases, the derivatives of $\bar{\mathcal{J}}^{\partial\Omega}$ appearing in (3.13) do not vanish. Recalling the definition of $\bar{\mathcal{J}}(\tilde{\boldsymbol{y}}, \boldsymbol{u})$ in (3.1), (2.8) and (2.11), we immediately get that for $\tilde{\boldsymbol{y}} = (\tilde{\boldsymbol{v}}, \tilde{p}^*, \tilde{\alpha})$ and $z \in \{\tilde{\boldsymbol{v}}, \tilde{p}^*, \tilde{\alpha}\}$

$$\bar{\mathcal{J}}_z(\tilde{\boldsymbol{y}}, \boldsymbol{u})[\delta z] = 2\{a_f \tilde{\boldsymbol{f}}(\tilde{\boldsymbol{y}}, \boldsymbol{u})^T \Theta_f \Theta_f^T \tilde{\boldsymbol{f}}_z(\tilde{\boldsymbol{y}}, \boldsymbol{u})[\delta z] + a_m \tilde{\boldsymbol{m}}(\tilde{\boldsymbol{y}}, \boldsymbol{u})^T \Theta_m \Theta_m^T \tilde{\boldsymbol{m}}_z(\tilde{\boldsymbol{y}}, \boldsymbol{u})[\delta z]\}.$$

Next, $\tilde{\boldsymbol{f}}_{\tilde{\boldsymbol{v}}}(\tilde{\boldsymbol{y}}, \boldsymbol{u})[\widetilde{\delta \boldsymbol{v}}] = \int_{\Gamma_{\boldsymbol{u},\mathrm{B}}} -\tilde{\mu}_{\mathrm{eff}}\, D(\widetilde{\delta \boldsymbol{v}})\tilde{\boldsymbol{n}}\, \mathrm{d}S$, $\tilde{\boldsymbol{f}}_{\tilde{p}}(\tilde{\boldsymbol{y}}, \boldsymbol{u})[\widetilde{\delta p}] = \int_{\Gamma_{\boldsymbol{u},\mathrm{B}}} (\widetilde{\delta p}\, \boldsymbol{I})\tilde{\boldsymbol{n}}\, \mathrm{d}S$ as well as

$$\begin{aligned}
\tilde{\boldsymbol{m}}_{\tilde{\boldsymbol{v}}}(\tilde{\boldsymbol{y}}, \boldsymbol{u})[\widetilde{\delta \boldsymbol{v}}] &= \int_{\Gamma_{\boldsymbol{u},\mathrm{B}}} (\tilde{\boldsymbol{x}} - \tilde{\boldsymbol{x}}_G) \times (-\tilde{\mu}_{\mathrm{eff}} D(\widetilde{\delta \boldsymbol{v}})\tilde{\boldsymbol{n}})\mathrm{d}S \\
\tilde{\boldsymbol{m}}_{\tilde{p}}(\tilde{\boldsymbol{y}}, \boldsymbol{u})[\widetilde{\delta p}] &= \int_{\Gamma_{\boldsymbol{u},\mathrm{B}}} (\tilde{\boldsymbol{x}} - \tilde{\boldsymbol{x}}_G) \times (\widetilde{\delta p}\, \boldsymbol{I})\tilde{\boldsymbol{n}}\, \mathrm{d}S.
\end{aligned}$$

Using $\tilde{\mu}_{\mathrm{eff}} = \tilde{\alpha}\mu_1 + (1 - \tilde{\alpha})\, \mu_2 + \tilde{\mu}_T$, we get

$$\begin{aligned}
\tilde{\boldsymbol{f}}_{\tilde{\alpha}}(\tilde{\boldsymbol{y}}, \boldsymbol{u})\, [\widetilde{\delta\alpha}] &= \int_{\Gamma_{\boldsymbol{u},\mathrm{B}}} \Big(\widetilde{\delta\alpha}\, (\tilde{\rho}_1 - \tilde{\rho}_2)\, \boldsymbol{g}^T \tilde{\boldsymbol{x}} \boldsymbol{I} - \widetilde{\delta\alpha}\, (\tilde{\mu}_1 - \tilde{\mu}_2)\, D(\nabla \tilde{\boldsymbol{v}})\Big) \tilde{\boldsymbol{n}}\, \mathrm{d}S, \\
\tilde{\boldsymbol{m}}_{\tilde{\alpha}}(\tilde{\boldsymbol{y}}, \boldsymbol{u})\, [\widetilde{\delta\alpha}] &= \int_{\Gamma_{\boldsymbol{u},\mathrm{B}}} (\tilde{\boldsymbol{x}} - \tilde{\boldsymbol{x}}_G) \times \big((\widetilde{\delta\alpha}\, (\tilde{\rho}_1 - \tilde{\rho}_2)\, \boldsymbol{g}^T \tilde{\boldsymbol{x}} \boldsymbol{I} - \widetilde{\delta\alpha}\, (\tilde{\mu}_1 - \tilde{\mu}_2)\, D(\nabla \tilde{\boldsymbol{v}}))\tilde{\boldsymbol{n}}\big)\, \mathrm{d}S.
\end{aligned}$$

Inserting these into (3.13a) and (3.13b) leads to

$$\int_{\Gamma_{\boldsymbol{u},\mathrm{B}}} \tilde{\boldsymbol{w}}^T \tilde{\mu}_{\text{eff}} (\nabla \widetilde{\delta \boldsymbol{v}})^T \tilde{\boldsymbol{n}} \, \mathrm{d}S = 2a_f \, \tilde{\boldsymbol{f}}(\tilde{\boldsymbol{y}}, \boldsymbol{u})^T \Theta_f \Theta_f^T \int_{\Gamma_{\boldsymbol{u},\mathrm{B}}} -\tilde{\mu}_{\text{eff}} D(\widetilde{\delta \boldsymbol{v}}) \tilde{\boldsymbol{n}} \, \mathrm{d}S + \\ + 2a_m \, \tilde{\boldsymbol{m}}(\tilde{\boldsymbol{y}}, \boldsymbol{u})^T \Theta_m \Theta_m^T \int_{\Gamma_{\boldsymbol{u},\mathrm{B}}} (\tilde{\boldsymbol{x}} - \tilde{\boldsymbol{x}}_G) \times \big(- \tilde{\mu}_{\text{eff}} D(\widetilde{\delta \boldsymbol{v}}) \tilde{\boldsymbol{n}} \big) \mathrm{d}S \tag{3.14}$$

$$\int_{\Gamma_{\boldsymbol{u},\mathrm{B}}} \widetilde{\delta p} \left(\tilde{\boldsymbol{w}}^T \tilde{\boldsymbol{n}} \right) \mathrm{d}S = -2a_f \tilde{\boldsymbol{f}}(\tilde{\boldsymbol{y}}, \boldsymbol{u})^T \Theta_f \Theta_f^T \int_{\Gamma_{\boldsymbol{u},\mathrm{B}}} \left(\widetilde{\delta p} \boldsymbol{I} \right) \tilde{\boldsymbol{n}} \, \mathrm{d}S \\ - 2a_m \tilde{\boldsymbol{m}}(\tilde{\boldsymbol{y}}, \boldsymbol{u})^T \Theta_m \Theta_m^T \int_{\Gamma_{\boldsymbol{u},\mathrm{B}}} (\tilde{\boldsymbol{x}} - \tilde{\boldsymbol{x}}_G) \times \left(\widetilde{\delta p} \boldsymbol{I} \right) \tilde{\boldsymbol{n}} \, \mathrm{d}S. \tag{3.15}$$

Next, we aim at proving that

$$\int_{\Gamma_{\boldsymbol{u},\mathrm{B}}} \tilde{\boldsymbol{w}}^T \tilde{\mu}_{\text{eff}} \nabla (\widetilde{\delta \boldsymbol{v}}) \, \tilde{\boldsymbol{n}} \, \mathrm{d}S = 0. \tag{3.16}$$

In fact, since $\widetilde{\delta \boldsymbol{v}}_{|\Gamma_{\boldsymbol{u},\mathrm{B}}} \equiv 0$, we obtain on $\Gamma_{\boldsymbol{u},\mathrm{B}}$ that $\nabla(\widetilde{\delta \boldsymbol{v}}) \, \tilde{\boldsymbol{n}} = \nabla(\widetilde{\delta \boldsymbol{v}}^T \tilde{\boldsymbol{n}}) - (\nabla \tilde{\boldsymbol{n}}) \widetilde{\delta \boldsymbol{v}} = \nabla(\widetilde{\delta v_n})$. Exactly as in §3.2.1, we get $\tilde{\boldsymbol{n}}^T (\nabla(\widetilde{\delta v_n})) = 0$. Then, by orthogonality of normal and tangential components we get

$$\tilde{\boldsymbol{w}}^T (\nabla(\widetilde{\delta \boldsymbol{v}}) \tilde{\boldsymbol{n}}) = \tilde{\boldsymbol{w}}^T (\nabla(\widetilde{\delta v_n})) = (\tilde{\boldsymbol{w}}_n^T + \tilde{\boldsymbol{w}}_t^T)(\nabla(\widetilde{\delta v_n})) = \tilde{\boldsymbol{w}}_n^T (\nabla(\widetilde{\delta v_n})) \\ = (\tilde{\boldsymbol{w}}^T \tilde{\boldsymbol{n}}) \tilde{\boldsymbol{n}}^T (\nabla(\widetilde{\delta v_n})) = 0,$$

i.e., (3.16). Now, we add this vanishing term to (3.14) and get

$$\int_{\Gamma_{\boldsymbol{u},\mathrm{B}}} \tilde{\boldsymbol{w}}^T \tilde{\mu}_{\text{eff}} (\nabla \widetilde{\delta \boldsymbol{v}})^T \tilde{\boldsymbol{n}} \, \mathrm{d}S = \int_{\Gamma_{\boldsymbol{u},\mathrm{B}}} \tilde{\boldsymbol{w}}^T \tilde{\mu}_{\text{eff}} \big(\nabla \widetilde{\delta \boldsymbol{v}} + (\nabla \widetilde{\delta \boldsymbol{v}})^T \big) \tilde{\boldsymbol{n}} \, \mathrm{d}S = \\ = \int_{\Gamma_{\boldsymbol{u},\mathrm{B}}} \tilde{\boldsymbol{w}}^T \tilde{\mu}_{\text{eff}} D(\widetilde{\delta \boldsymbol{v}}) \tilde{\boldsymbol{n}} \, \mathrm{d}S \\ = 2a_f \tilde{\boldsymbol{f}}(\tilde{\boldsymbol{y}}, \boldsymbol{u})^T \Theta_f \Theta_f^T \int_{\Gamma_{\boldsymbol{u},\mathrm{B}}} -\tilde{\mu}_{\text{eff}} D(\widetilde{\delta \boldsymbol{v}}) \tilde{\boldsymbol{n}} \, \mathrm{d}S \\ + 2a_m \tilde{\boldsymbol{m}}(\tilde{\boldsymbol{y}}, \boldsymbol{u})^T \Theta_m \Theta_m^T \int_{\Gamma_{\boldsymbol{u},\mathrm{B}}} (\tilde{\boldsymbol{x}} - \tilde{\boldsymbol{x}}_G) \times \left(-\tilde{\mu}_{\text{eff}} D(\widetilde{\delta \boldsymbol{v}}) \tilde{\boldsymbol{n}} \right) \mathrm{d}S. \tag{3.17}$$

Using $\boldsymbol{u}^T (\boldsymbol{v} \times \boldsymbol{w}) = (\boldsymbol{u} \times \boldsymbol{v})^T \boldsymbol{w}$ we now obtain the boundary condition

$$\tilde{\boldsymbol{w}}(\tilde{\boldsymbol{x}}) = -2a_f \Theta_f \Theta_f^T \tilde{\boldsymbol{f}}(\tilde{\boldsymbol{y}}, \boldsymbol{u}) - 2a_m \left(\Theta_m \Theta_m^T \tilde{\boldsymbol{m}}(\tilde{\boldsymbol{y}}, \boldsymbol{u}) \right) \times (\tilde{\boldsymbol{x}} - \tilde{\boldsymbol{x}}_G), \qquad \tilde{\boldsymbol{x}} \in \Gamma_{\boldsymbol{u},\mathrm{B}}.$$

Starting at (3.15) yields exactly the same condition.

Remark 3.5. *If we would have an objective function including only forces, we would get a constant Dirichlet boundary condition for* $\tilde{\boldsymbol{w}}$. *However, if moments are also involved, the boundary condition depends on the specific position of* $\tilde{\boldsymbol{x}} \in \Gamma_{\boldsymbol{u},\mathrm{B}}$. □

Like for the preceding paragraphs, we do not obtain a boundary condition on $\tilde{q}$ and therefore we choose a Neumann condition:

$$\nabla \tilde{q}^T \tilde{\boldsymbol{n}} = 0, \qquad \forall \tilde{\boldsymbol{x}} \in \Gamma_{\boldsymbol{u},\mathrm{wall}}.$$

3.2.4. Outlet Boundaries. Finally, we consider the outlet boundary $\Gamma_{\boldsymbol{u},\text{out}}$. It turns out to be quite convenient to assume planar boundary patches of $\Gamma_{\boldsymbol{u},\text{out}}$, i.e., $\nabla\tilde{\boldsymbol{n}} = 0$ and $\nabla\tilde{\boldsymbol{t}}$ for any tangential vector $\tilde{\boldsymbol{t}}$. Moreover, we assume that $\Gamma_{\boldsymbol{u},\text{out}}$ is located in the far field, so that we may assume $\nabla\tilde{\mu}_T = 0$, where $\tilde{\mu}_{\text{eff}} = \tilde{\mu} + \tilde{\mu}_T$.

We are now going to derive the corresponding boundary conditions. First, for $\tilde{\boldsymbol{y}} + \widetilde{\delta\boldsymbol{y}} \in Y(\Omega_{\boldsymbol{u}})$, $\widetilde{\delta\boldsymbol{y}} = (\widetilde{\delta\boldsymbol{w}}, \widetilde{\delta p}, \widetilde{\delta\alpha})$, we obtain

$$(\tilde{\boldsymbol{n}}\cdot\nabla)\widetilde{\delta\boldsymbol{w}} = \nabla(\widetilde{\delta\boldsymbol{w}})^T\tilde{\boldsymbol{n}} = 0, \qquad \widetilde{\delta p} = 0, \qquad (\widetilde{\delta\alpha})^T\tilde{\boldsymbol{n}} = 0, \qquad \text{on } \Gamma_{\boldsymbol{u},\text{out}}.$$

Since $\widetilde{\delta p}_{|\Gamma_{\boldsymbol{u},\text{out}}} = 0$, the equation (3.6b) is always satisfied. With the application of Lemma 3.4 the remaining conditions in (3.6) reduce to

$$\begin{aligned}&\int_{\Gamma_{\boldsymbol{u},\text{out}}} \{\widetilde{\delta\boldsymbol{v}}^T\left(\tilde{\rho}\,\tilde{\boldsymbol{n}}\tilde{\boldsymbol{w}}^T\tilde{\boldsymbol{v}} + \tilde{\rho}\tilde{\boldsymbol{w}}\tilde{\boldsymbol{v}}^T\tilde{\boldsymbol{n}} + \tilde{\mu}_{\text{eff}}(\nabla\tilde{\boldsymbol{w}})^T\tilde{\boldsymbol{n}} + \tilde{\boldsymbol{n}}\,\tilde{q} + \tilde{\alpha}\tilde{\gamma}\,\tilde{\boldsymbol{n}}\right) - \\ &\qquad -\tilde{\boldsymbol{w}}^T\tilde{\mu}_{\text{eff}}(\nabla(\widetilde{\delta\boldsymbol{v}}))^T\tilde{\boldsymbol{n}} - \nabla\tilde{\mu}_{\text{eff}}^T\left(\tilde{w}_n\widetilde{\delta\boldsymbol{v}} - \widetilde{\delta v_n}\tilde{\boldsymbol{w}}\right)\}\mathrm{d}S = 0,\end{aligned} \tag{3.18a}$$

$$\begin{aligned}&\int_{\Gamma_{\boldsymbol{u},\text{out}}} \widetilde{\delta\alpha}\big(-(\tilde{\mu}_1 - \tilde{\mu}_2)\,\tilde{\boldsymbol{w}}^T(\nabla\tilde{\boldsymbol{v}})\tilde{\boldsymbol{n}} + (\tilde{\rho}_1 - \tilde{\rho}_2)\,\tilde{\boldsymbol{w}}^T\tilde{\boldsymbol{v}}\tilde{\boldsymbol{v}}^T\tilde{\boldsymbol{n}} + \\ &\qquad + (\tilde{\rho}_1 - \tilde{\rho}_2)\,\boldsymbol{g}^T\tilde{\boldsymbol{x}}\tilde{\boldsymbol{w}}^T\tilde{\boldsymbol{n}} + \tilde{\gamma}\tilde{\boldsymbol{v}}^T\tilde{\boldsymbol{n}}\big)\,\mathrm{d}S = 0.\end{aligned} \tag{3.18b}$$

Next, we will simplify (3.18a). First, note that $\nabla\tilde{\mu}_{\text{eff}} = \nabla\tilde{\mu} + \nabla\tilde{\mu}_T = \nabla(\tilde{\alpha}_1\tilde{\mu}_1 + (1 - \tilde{\alpha})\tilde{\mu}_2) = (\tilde{\mu}_1 - \tilde{\mu}_2)\nabla\tilde{\alpha}$. Then, recall that $\widetilde{\delta\boldsymbol{y}} \in Y(\Omega_{\boldsymbol{u}})$, which implies that from the primal problem we observe that

$$\nabla\cdot\widetilde{\delta\boldsymbol{v}} = 0, \qquad \nabla\cdot(\tilde{\alpha}\,\widetilde{\delta\boldsymbol{v}}) = 0, \qquad \tilde{\boldsymbol{n}}^T(\nabla\tilde{\alpha}) = 0 \qquad \text{on } \Gamma_{\boldsymbol{u},\text{out}}.$$

Hence, on $\Gamma_{\boldsymbol{u},\text{out}}$, it holds that $0 = \nabla\cdot(\tilde{\alpha}\,\widetilde{\delta\boldsymbol{v}}) = (\nabla\tilde{\alpha})^T(\widetilde{\delta\boldsymbol{v}}) + \tilde{\alpha}(\nabla\cdot\widetilde{\delta\boldsymbol{v}}) = (\nabla\tilde{\alpha})^T(\widetilde{\delta\boldsymbol{v}})$. The next step is

$$\begin{aligned}(\nabla\tilde{\mu}_{\text{eff}})^T(\tilde{w}_n\,\widetilde{\delta\boldsymbol{v}} - (\widetilde{\delta v_n})\tilde{\boldsymbol{w}}) &= (\tilde{\mu}_1 - \tilde{\mu}_2)(\nabla\tilde{\alpha})^T(\tilde{w}_n\,\widetilde{\delta\boldsymbol{v}} - (\widetilde{\delta v_n})\tilde{\boldsymbol{w}}) \\ &= -(\tilde{\mu}_1 - \tilde{\mu}_2)(\nabla\tilde{\alpha})^T(\widetilde{\delta v_n})\tilde{\boldsymbol{w}} = (\tilde{\mu}_2 - \tilde{\mu}_1)((\widetilde{\delta\boldsymbol{v}})^T\tilde{\boldsymbol{n}})(\nabla\tilde{\alpha})^T\tilde{\boldsymbol{w}}_t,\end{aligned}$$

where the last step follows from $(\nabla\tilde{\alpha})^T\tilde{\boldsymbol{w}}_n = \tilde{w}_n(\nabla\tilde{\alpha})^T\tilde{\boldsymbol{n}} = 0$ on $\Gamma_{\boldsymbol{u},\text{out}}$. Hence, (3.18a) is equivalent to

$$\int_{\Gamma_{\boldsymbol{u},\text{out}}} (\widetilde{\delta\boldsymbol{v}})^T\{\left(\tilde{\rho}\,\tilde{\boldsymbol{w}}^T\tilde{\boldsymbol{v}} + \tilde{q} + \tilde{\alpha}\tilde{\gamma} + (\tilde{\mu}_1 - \tilde{\mu}_2)(\nabla\tilde{\alpha})^T\tilde{\boldsymbol{w}}_t\right)\tilde{\boldsymbol{n}} + \tilde{\mu}_{\text{eff}}(\nabla\tilde{\boldsymbol{w}})^T\tilde{\boldsymbol{n}} + \tilde{\rho}\tilde{v}_n\tilde{\boldsymbol{w}}\}\mathrm{d}S = 0$$

for all $\widetilde{\delta\boldsymbol{v}}$ such that $\widetilde{\delta\boldsymbol{y}} \in Y(\Omega_{\boldsymbol{u}})$. Thus, the term in $\{\cdots\}$ vanishes, i.e, on $\Gamma_{\boldsymbol{u},\text{out}}$,

$$0 = \left(\tilde{\rho}\,\tilde{\boldsymbol{w}}^T\tilde{\boldsymbol{v}} + \tilde{q} + \tilde{\alpha}\tilde{\gamma} + (\tilde{\mu}_1 - \tilde{\mu}_2)(\nabla\tilde{\alpha})^T\tilde{\boldsymbol{w}}_t\right)\tilde{\boldsymbol{n}} + \tilde{\mu}_{\text{eff}}(\nabla\tilde{\boldsymbol{w}})^T\tilde{\boldsymbol{n}} + \tilde{\rho}\tilde{v}_n\tilde{\boldsymbol{w}}. \tag{3.19}$$

Using the same reasoning to (3.18b) yields

$$0 = (\tilde{\mu}_2 - \tilde{\mu}_1)\tilde{\boldsymbol{w}}^T(\nabla\tilde{\boldsymbol{v}})\tilde{\boldsymbol{n}} + (\tilde{\rho}_1 - \tilde{\rho}_2)[\tilde{\boldsymbol{w}}^T\tilde{\boldsymbol{v}}\tilde{\boldsymbol{v}}^T + \boldsymbol{g}^T\tilde{\boldsymbol{x}}\tilde{\boldsymbol{w}}^T]\tilde{\boldsymbol{n}} + \tilde{\gamma}(\tilde{\boldsymbol{v}}^T\tilde{\boldsymbol{n}}). \tag{3.20}$$

Since (possibly by modifying the position of $\Gamma_{\boldsymbol{u},\text{out}}$) we may assume that $\tilde{\boldsymbol{v}}^T\tilde{\boldsymbol{n}} = \tilde{v}_n \neq 0$ on $\Gamma_{\boldsymbol{u},\text{out}}$, we obtain from (3.20)

$$\tilde{\gamma} = \frac{1}{\tilde{\boldsymbol{v}}^T\tilde{\boldsymbol{n}}}\{(\tilde{\mu}_1 - \tilde{\mu}_2)\,\tilde{\boldsymbol{w}}^T\,(\nabla\tilde{\boldsymbol{v}})\,\tilde{\boldsymbol{n}} - (\tilde{\rho}_1 - \tilde{\rho}_2)\left(\tilde{\boldsymbol{w}}^T\tilde{\boldsymbol{v}}\tilde{\boldsymbol{v}}^T\tilde{\boldsymbol{n}} + \boldsymbol{g}^T\tilde{\boldsymbol{x}}\tilde{\boldsymbol{w}}^T\tilde{\boldsymbol{n}}\right)\}. \tag{3.21}$$

Obviously, the latter one is a scalar equation, wheres (3.19) is vector-valued. Hence, we consider normal and tangential parts of this equation. Taking the inner product with any tangential vector $\tilde{\boldsymbol{t}}$ (i.e, $\tilde{\boldsymbol{n}}^T\tilde{\boldsymbol{t}} = 0$) yields

$$\tilde{\rho}\tilde{v}_n\tilde{w}_t + \tilde{\mu}_{\text{eff}}(\nabla\tilde{w}_t)^T\tilde{\boldsymbol{n}} = 0 \tag{3.22}$$

since $((\nabla\tilde{\boldsymbol{w}})\tilde{\boldsymbol{n}})^T\tilde{\boldsymbol{t}} = \tilde{\boldsymbol{n}}(\nabla\tilde{\boldsymbol{w}})^T\tilde{\boldsymbol{t}} = (\nabla\tilde{w}_t)^T\tilde{\boldsymbol{n}}$. For the normal component, we get

$$0 = \tilde{\rho}\tilde{\boldsymbol{w}}^T\tilde{\boldsymbol{v}} + \tilde{q} + \tilde{\alpha}\tilde{\gamma} + (\tilde{\mu}_1 - \tilde{\mu}_2)(\nabla\tilde{\alpha})^T\tilde{\boldsymbol{w}}_t + \tilde{\rho}\tilde{v}_n\tilde{w}_n + \tilde{\mu}_{\text{eff}}(\nabla\tilde{w}_n)^T\tilde{\boldsymbol{n}}, \tag{3.23}$$

where the last term can be seen as follows (using $\nabla\tilde{\boldsymbol{n}} = 0$)

$$((\nabla\tilde{\boldsymbol{w}})^T\tilde{\boldsymbol{n}})^T\tilde{\boldsymbol{n}} = \tilde{\boldsymbol{n}}^T(\nabla\tilde{\boldsymbol{w}})\tilde{\boldsymbol{n}} = \tilde{\boldsymbol{n}}^T(\nabla\tilde{w}_n) = (\nabla\tilde{w}_n)^T\tilde{\boldsymbol{n}}.$$

Altogether, we obtain the boundary conditions (3.21), (3.22) and (3.23) on $\Gamma_{\boldsymbol{u},\text{out}}$. The tangential part of $\tilde{\boldsymbol{w}}$, i.e., $\tilde{\boldsymbol{w}}_t$ is determined by (3.22), the adjoint phase fraction $\tilde{\gamma}$ by (3.21) and the adjoint pressure $\boldsymbol{q}$ by (3.23), where, however, the last two equations require the knowledge also of $\tilde{\boldsymbol{w}}_n$, which is determined by the pde-system using the adjoint flux.

3.2.5. Multiphase adjoint boundary conditions. Collecting the previous findings, we obtain the following multiphase adjoint boundary conditions:

$$\tilde{\boldsymbol{w}}_n = 0, \quad (\tilde{\boldsymbol{n}}\cdot\nabla)\,\tilde{\boldsymbol{w}}_t = 0, \quad \nabla\tilde{q}^T\tilde{\boldsymbol{n}} = 0, \quad \nabla\tilde{\gamma}^T\tilde{\boldsymbol{n}} = 0, \text{ on } \Gamma_{\boldsymbol{u},\text{in}}, \tag{3.24a}$$

$$\tilde{\gamma}_{\text{in}} = (\tilde{\mu}_1 - \tilde{\mu}_2)\,\tilde{\boldsymbol{w}}^T D(\nabla\tilde{\boldsymbol{v}}_{\text{in}})\tilde{\boldsymbol{n}} - (\tilde{\rho}_1 - \tilde{\rho}_2)\,\tilde{\boldsymbol{w}}^T\tilde{\boldsymbol{v}}_{\text{in}}\tilde{\boldsymbol{v}}_{\text{in}}^T\tilde{\boldsymbol{n}} - \tilde{\gamma}\tilde{\boldsymbol{v}}_{\text{in}}^T\tilde{\boldsymbol{n}}, \text{ on } \Gamma_{\boldsymbol{u},\text{in}}, \tag{3.24b}$$

$$\tilde{\boldsymbol{w}} = 0, \quad \nabla\tilde{q}^T\tilde{\boldsymbol{n}} = 0, \quad \nabla\tilde{\gamma}^T\tilde{\boldsymbol{n}} = 0, \text{ on } \Gamma_{\boldsymbol{u},\text{wall}}, \tag{3.24c}$$

$$\tilde{\boldsymbol{w}} = -2a_f\Theta_f\Theta_f^T\tilde{\boldsymbol{f}}\,(\tilde{\boldsymbol{y}},\boldsymbol{u}) - 2a_m\left(\Theta_m\Theta_m^T\tilde{\boldsymbol{m}}\,(\tilde{\boldsymbol{y}},\boldsymbol{u})\right)\times(\tilde{\boldsymbol{x}} - \tilde{\boldsymbol{x}}_G)\,, \text{ on } \Gamma_{\boldsymbol{u},\text{B}},$$

$$\nabla\tilde{q}^T\tilde{\boldsymbol{n}} = 0, \quad \nabla\tilde{\gamma}^T\tilde{\boldsymbol{n}} = 0, \text{ on } \Gamma_{\boldsymbol{u},\text{B}}, \tag{3.24d}$$

$$\tilde{\rho}\tilde{v}_n\tilde{\boldsymbol{w}}_t + \tilde{\mu}_{\text{eff}}\,(\nabla\tilde{\boldsymbol{w}}_t)^T\,\tilde{\boldsymbol{n}} = 0, \text{ on } \Gamma_{\boldsymbol{u},\text{out}}, \tag{3.24e}$$

$$\tilde{q} = -\tilde{\rho}\tilde{\boldsymbol{w}}^T\tilde{\boldsymbol{v}} - \tilde{\rho}\tilde{w}_n\tilde{v}_n - \tilde{\mu}_{\text{eff}}\,(\nabla\tilde{w}_n)^T\,\tilde{\boldsymbol{n}} - \tilde{\alpha}\tilde{\gamma} - (\tilde{\mu}_1 - \tilde{\mu}_2)\,\nabla\tilde{\alpha}^T\tilde{\boldsymbol{w}}_t \text{ on } \Gamma_{\boldsymbol{u},\text{out}}, \tag{3.24f}$$

$$\tilde{\gamma} = \frac{(\tilde{\mu}_1 - \tilde{\mu}_2)\,\tilde{\boldsymbol{w}}^T\,(\nabla\tilde{\boldsymbol{v}})\,\tilde{\boldsymbol{n}} - (\tilde{\rho}_1 - \tilde{\rho}_2)\left(\tilde{\boldsymbol{w}}^T\tilde{\boldsymbol{v}}\tilde{\boldsymbol{v}}^T\tilde{\boldsymbol{n}} + \boldsymbol{g}^T\tilde{\boldsymbol{x}}\tilde{\boldsymbol{w}}^T\tilde{\boldsymbol{n}}\right)}{\tilde{\boldsymbol{v}}^T\tilde{\boldsymbol{n}}}, \text{ on } \Gamma_{\boldsymbol{u},\text{out}}. \tag{3.24g}$$

3.3. Parameter Derivatives. In the last step of our general procedure, we have to determine the derivative of the reduced cost function

$$j_{\boldsymbol{u}}\,(\boldsymbol{u})\,[\delta\boldsymbol{u}] = \langle\bar{\mathcal{J}}_{\boldsymbol{u}}\,(\tilde{\boldsymbol{y}},\boldsymbol{u})^T\,,\delta\boldsymbol{u}\rangle_{U^*,U} + \langle\tilde{\boldsymbol{\lambda}},\bar{\mathcal{R}}_{\boldsymbol{u}}\,(\tilde{\boldsymbol{y}},\boldsymbol{u})\,\delta\boldsymbol{u}\rangle_{Z(\Omega_{\boldsymbol{u}})^*,Z(\Omega_{\boldsymbol{u}})},$$

with the solution $\tilde{\boldsymbol{y}} = (\tilde{\boldsymbol{v}},\tilde{p}^*,\tilde{\alpha})$ of the multiphase Navier-Stokes equations (2.3) which is equivalent to the solution of the stationary system (2.4) for converged flow variables and the solution $\tilde{\boldsymbol{\lambda}} = (\tilde{\boldsymbol{w}},\tilde{q},\tilde{\gamma},\tilde{\gamma}_{\text{in}})$ of the corresponding adjoint system (3.5) with adjoint boundary conditions (3.24) for given $\boldsymbol{u}\in U_{\text{ad}}$.

We start with the transformation of the multiphase constraint system to the reference domain and its differentiation w.r.t. $\boldsymbol{u}$. Then, we present the transformation and differentiation of the multiphase objective function.

3.3.1. Multiphase Constraint System. Using standard formulas for changing variables in integration, we get

$$\langle\tilde{\boldsymbol{\lambda}},\bar{\mathcal{R}}\,(\tilde{\boldsymbol{y}},\boldsymbol{u})\rangle_{Z(\Omega_{\boldsymbol{u}})^*,Z(\Omega_{\boldsymbol{u}})} = \langle(\tilde{\boldsymbol{w}},\tilde{q},\tilde{\gamma},\tilde{\gamma}_{\text{in}}),\bar{\mathcal{R}}\,((\tilde{\boldsymbol{v}},\tilde{p}^*,\tilde{\alpha})\,,\boldsymbol{u})\rangle_{Z(\Omega_{\boldsymbol{u}})^*,Z(\Omega_{\boldsymbol{u}})}$$

$$
\begin{aligned}
&= \int_{\Omega_{\boldsymbol{u}}} \tilde{\boldsymbol{w}}^T \left(\tilde{\rho} \left(\tilde{\boldsymbol{v}} \cdot \nabla \right) \tilde{\boldsymbol{v}} + \nabla \tilde{p}^* - \nabla \cdot \left(\tilde{\mu}_{\text{eff}} \nabla \tilde{\boldsymbol{v}} \right) + \boldsymbol{g}^T \tilde{\boldsymbol{x}} \nabla \tilde{\rho} \right) \mathrm{d}\tilde{\boldsymbol{x}} + \int_{\Omega_{\boldsymbol{u}}} \tilde{q} \nabla \cdot \tilde{\boldsymbol{v}} \; \mathrm{d}\tilde{\boldsymbol{x}} \\
&\quad + \int_{\Omega_{\boldsymbol{u}}} \tilde{\gamma} \left(\tilde{\boldsymbol{v}} \cdot \nabla \right) \tilde{\alpha} \mathrm{d}\tilde{\boldsymbol{x}} + \int_{\Gamma_{\boldsymbol{u},\text{in}}} \tilde{\gamma}_{\text{in}} \left(\tilde{\alpha} - \tilde{\alpha}_{\text{in}} \right) \mathrm{d}S \\
&= \int_{\Omega_{\text{ref}}} \boldsymbol{w}^T \Bigg\{ \nabla \boldsymbol{v}^T ((\nabla \boldsymbol{\tau}^{\boldsymbol{u}})^{-1})^T \boldsymbol{v} + \left(\nabla \boldsymbol{\tau}^{\boldsymbol{u}} \right)^{-1} \nabla p^* - \nabla \boldsymbol{v}^T \left(\nabla \boldsymbol{\tau}^{\boldsymbol{u}} \right)^{-T} \left(\nabla \boldsymbol{\tau}^{\boldsymbol{u}} \right)^{-1} \nabla \mu_{\text{eff}} \\
&\qquad - \mu_{\text{eff}} \left[\nabla \boldsymbol{v}^T \Delta_{\tilde{\boldsymbol{x}}} ((\boldsymbol{\tau}^{\boldsymbol{u}})^{-1}) + \left(\operatorname{tr}\{ H\left(v_j \right) \left(\nabla \boldsymbol{\tau}^{\boldsymbol{u}} \right)^{-T} \left(\nabla \boldsymbol{\tau}^{\boldsymbol{u}} \right)^{-1} \} \right)_{j=1}^{d} \right] \\
&\qquad\qquad + \boldsymbol{g}^T \boldsymbol{\tau}^{\boldsymbol{u}} \left(\boldsymbol{x} \right) \left(\nabla \boldsymbol{\tau}^{\boldsymbol{u}} \right)^{-1} \nabla \rho \Bigg\} \left| \det J_{\boldsymbol{\tau}^{\boldsymbol{u}}} \left(\boldsymbol{x} \right) \right| \mathrm{d}\boldsymbol{x} \\
&\quad + \int_{\Omega_{\text{ref}}} \left\{ q \operatorname{tr} \left(\left(\nabla \boldsymbol{\tau}^{\boldsymbol{u}} \right)^{-1} \nabla \boldsymbol{v} \right) + \gamma \nabla \alpha^T \left(\nabla \boldsymbol{\tau}^{\boldsymbol{u}} \right)^{-T} \boldsymbol{v} \right\} \left| \det J_{\boldsymbol{\tau}^{\boldsymbol{u}}} \left(\boldsymbol{x} \right) \right| \mathrm{d}\boldsymbol{x} \\
&\quad + \int_{\Gamma_{\text{ref,in}}} \gamma_{\text{in}} \left(\alpha - \tilde{\alpha}_{\text{in}} \left(\boldsymbol{\tau}^{\boldsymbol{u}} \left(\boldsymbol{x} \right) \right) \right) \left| \det J_{\boldsymbol{\tau}^{\boldsymbol{u}}} \left(\boldsymbol{x} \right) \right| \mathrm{d}S =: \langle (\boldsymbol{w}, q, \gamma), \mathcal{R}\left(\left(\boldsymbol{v}, p, \alpha \right), \boldsymbol{u} \right) \rangle_{Z_{\text{ref}}^*, Z_{\text{ref}}}
\end{aligned}
$$

with

$$
\mathcal{R}\left(\left(\boldsymbol{v}, p, \alpha \right), \boldsymbol{u} \right) = \\
= \begin{pmatrix}
\Big[\nabla \boldsymbol{v}^T \left(\nabla \boldsymbol{\tau}^{\boldsymbol{u}} \right)^{-T} \boldsymbol{v} + \left(\nabla \boldsymbol{\tau}^{\boldsymbol{u}} \right)^{-1} \nabla p^* - \nabla \boldsymbol{v}^T \left(\nabla \boldsymbol{\tau}^{\boldsymbol{u}} \right)^{-T} \left(\nabla \boldsymbol{\tau}^{\boldsymbol{u}} \right)^{-1} \nabla \mu_{\text{eff}} \\
\quad - \mu_{\text{eff}} \Big\{ \nabla \boldsymbol{v}^T \Delta_{\tilde{\boldsymbol{x}}} \left(\left(\boldsymbol{\tau}^{\boldsymbol{u}} \right)^{-1} \right) + \left[\operatorname{tr} \left(H\left(v_j \right) \left(\nabla \boldsymbol{\tau}^{\boldsymbol{u}} \right)^{-T} \left(\nabla \boldsymbol{\tau}^{\boldsymbol{u}} \right)^{-1} \right) \right]_{j=1}^{d} \Big\} \\
\quad + \boldsymbol{g}^T \boldsymbol{\tau}^{\boldsymbol{u}} \left(\boldsymbol{x} \right) \left(\nabla \boldsymbol{\tau}^{\boldsymbol{u}} \right)^{-1} \nabla \rho \Big] \left| \det J_{\boldsymbol{\tau}^{\boldsymbol{u}}} \left(\boldsymbol{x} \right) \right| \\
\operatorname{tr} \left(\left(\nabla \boldsymbol{\tau}^{\boldsymbol{u}} \right)^{-1} \nabla \boldsymbol{v} \right) \left| \det J_{\boldsymbol{\tau}^{\boldsymbol{u}}} \left(\boldsymbol{x} \right) \right| \\
\nabla \alpha^T \left(\nabla \boldsymbol{\tau}^{\boldsymbol{u}} \right)^{-T} \boldsymbol{v} \left| \det J_{\boldsymbol{\tau}^{\boldsymbol{u}}} \left(\boldsymbol{x} \right) \right| \\
\gamma_{\text{in}} \left(\alpha - \tilde{\alpha}_{\text{in}} \left(\boldsymbol{\tau}^{\boldsymbol{u}} \left(\boldsymbol{x} \right) \right) \right) \left| \det J_{\boldsymbol{\tau}^{\boldsymbol{u}}} \left(\boldsymbol{x} \right) \right|
\end{pmatrix}
$$

Note, that we kept the "~" for the phase fraction inlet value $\tilde{\alpha}_{\text{in}} \left(\boldsymbol{\tau}^{\boldsymbol{u}} \left(\boldsymbol{x} \right) \right)$. This is due to the fact that this variable is a given input function and not the result of the flow calculation. Therefore its dependency on $\boldsymbol{u}$ is explicit and not implicit through the state equations. This is relevant for the derivative w.r.t. $\boldsymbol{u}$ later. By using standard arguments for differentiation (see [27, §4.3.2, 5.3.1] for details), we then obtain

(3.25a)

$$
\begin{aligned}
&\langle \nabla_{\boldsymbol{u}} \mathcal{R}\left(\left(\boldsymbol{v}, p^*, \alpha \right), \boldsymbol{u} \right), \left(\boldsymbol{w}, q, \gamma, \gamma_{\text{in}} \right) \rangle_{Z_{\text{ref}}, Z_{\text{ref}}^*} = \\
&= \int_{\Omega_{\text{ref}}} \Bigg\{ \Bigg[\rho \left(\boldsymbol{v}^T \left(\frac{\partial}{\partial u_i} \left(\nabla \boldsymbol{\tau}^{\boldsymbol{u}} \right)^{-1} \right) \right)_{i=1}^{n} \nabla \boldsymbol{v} + \left(\nabla p^{*T} \left(\frac{\partial}{\partial u_i} \left(\nabla \boldsymbol{\tau}^{\boldsymbol{u}} \right)^{-T} \right) \right)_{i=1}^{n} \\
&\qquad - \left[\nabla \mu_{\text{eff}}^T \left(\left(\frac{\partial}{\partial u_i} \left(\nabla \boldsymbol{\tau}^{\boldsymbol{u}} \right)^{-T} \right) \left(\nabla \boldsymbol{\tau}^{\boldsymbol{u}} \right)^{-1} + \left(\nabla \boldsymbol{\tau}^{\boldsymbol{u}} \right)^{-T} \left(\frac{\partial}{\partial u_i} \left(\nabla \boldsymbol{\tau}^{\boldsymbol{u}} \right)^{-1} \right) \right) \nabla \boldsymbol{v} \right]_{i=1}^{n} \\
&\qquad - \mu_{\text{eff}} \Bigg[\left(\nabla_{\boldsymbol{u}} \left(\Delta_{\tilde{\boldsymbol{x}}} \left(\left(\boldsymbol{\tau}^{\boldsymbol{u}} \right)^{-1} \right) \right) \nabla \boldsymbol{v} \right) + \Bigg(\Bigg[\operatorname{tr} \Bigg\{ H\left(v_j \right) \Bigg(\frac{\partial \left(\nabla \boldsymbol{\tau}^{\boldsymbol{u}} \right)^{-T}}{\partial u_i} \left(\nabla \boldsymbol{\tau}^{\boldsymbol{u}} \right)^{-1} + \\
&\qquad\qquad + \left(\nabla \boldsymbol{\tau}^{\boldsymbol{u}} \right)^{-T} \frac{\partial \left(\nabla \boldsymbol{\tau}^{\boldsymbol{u}} \right)^{-1}}{\partial u_i} \Bigg) \Bigg\} \Bigg]_{i=1}^{n} \Bigg)_{j=1,\ldots,d} \Bigg] +
\end{aligned}
$$

$$+\left\{\nabla\rho^T\Big(\big(\frac{\partial}{\partial u_i}\left(\nabla\boldsymbol{\tau}^{\boldsymbol{u}}\right)^{-T}\big)\boldsymbol{\tau}^{\boldsymbol{u}}\left(\boldsymbol{x}\right)^T\boldsymbol{g}+\right.$$

$$\left.\left.+\left(\nabla\boldsymbol{\tau}^{\boldsymbol{u}}\right)^{-T}\Big(\frac{\partial}{\partial u_i}\boldsymbol{\tau}^{\boldsymbol{u}}\left(\boldsymbol{x}\right)\Big)^T\boldsymbol{g}\Big)\right]_{i=1}^n\right\}\left|\det J_{\boldsymbol{\tau}^{\boldsymbol{u}}}\left(\boldsymbol{x}\right)\right|\Bigg\}\boldsymbol{w}\,\mathrm{d}\boldsymbol{x}$$

$$+\int_{\Omega_{\mathrm{ref}}}\left|\det J_{\boldsymbol{\tau}^{\boldsymbol{u}}}\left(\boldsymbol{x}\right)\right|\left(\left[\operatorname{tr}\left(\frac{\partial\left(\nabla\boldsymbol{\tau}^{\boldsymbol{u}}\right)^{-1}}{\partial u_i}\nabla\boldsymbol{v}\right)\right]_{i=1}^n q+\left[\nabla\alpha^T\frac{\partial}{\partial u_i}\left(\nabla\boldsymbol{\tau}^{\boldsymbol{u}}\right)^{-T}\right]_{i=1}^n\boldsymbol{v}\gamma\right)\mathrm{d}\boldsymbol{x}$$

$$-\int_{\Gamma_{\mathrm{ref,in}}}\left[\nabla_{\tilde{\boldsymbol{x}}}\tilde{\alpha}_{\mathrm{in}}\left(\boldsymbol{\tau}^{\boldsymbol{u}}\left(\boldsymbol{x}\right)\right)^T\frac{\partial}{\partial u_i}\boldsymbol{\tau}^{\boldsymbol{u}}\left(\boldsymbol{x}\right)\right]_{i=1}^n\left|\det J_{\boldsymbol{\tau}^{\boldsymbol{u}}}\left(\boldsymbol{x}\right)\right|\gamma_{\mathrm{in}}\,\mathrm{d}\boldsymbol{x}.$$

REMARK 3.6. *In the above calculations, we assumed two fluids with a* smooth *phase fraction. i.e., a C^2-transition area of finite thickness. This is relevant for the differentiation of the phase fraction variable α and its inlet condition $\tilde{\alpha}_{\mathrm{in}}\left(\boldsymbol{\tau}^{\boldsymbol{u}}\left(\boldsymbol{x}\right)\right)$ as the term $-\int_{\Omega_{\mathrm{ref}}}\left[\nabla_{\tilde{\boldsymbol{x}}}\tilde{\alpha}_{\mathrm{in}}\left(\boldsymbol{\tau}^{\boldsymbol{u}}\left(\boldsymbol{x}\right)\right)^T\frac{\partial}{\partial u_i}\boldsymbol{\tau}^{\boldsymbol{u}}\left(\boldsymbol{x}\right)\right]_{i=1}^n\left|\det J_{\boldsymbol{\tau}^{\boldsymbol{u}}}\left(\boldsymbol{x}\right)\right|\gamma_{\mathrm{in}}\,\mathrm{d}\boldsymbol{x}$ is only nonzero in the very small transition area of the interface.*

However, this transition area should be small which induces steep gradients that may not be resolvable by the numerical scheme. This, in turn might cause errors in the gradient of the objective function. If the discretization cannot be chosen sufficiently fine to reproduce such steep gradients, it might be better to neglect the corresponding terms as the numerical error might exceed the modeling error by neglecting its contribution. □

3.3.2. Multiphase Objective Function. For the transformation of the terms $\boldsymbol{f}\left(\left(\boldsymbol{v},p^*,\alpha\right),\boldsymbol{u}\right)$ and $\boldsymbol{m}\left(\left(\boldsymbol{v},p^*,\alpha\right),\boldsymbol{u}\right)$ a change of variables gives

$$\boldsymbol{f}\left(\left(\boldsymbol{v},p^*,\alpha\right),\boldsymbol{u}\right)=\int_{\Gamma_{\mathrm{ref,B}}}\Big(\left(\tilde{p}^*+\rho\boldsymbol{g}^T\boldsymbol{\tau}^{\boldsymbol{u}}\left(\boldsymbol{x}\right)\right)I-\mu_{\mathrm{eff}}\big[\left(\left(\nabla\boldsymbol{\tau}^{\boldsymbol{u}}\right)^{-1}\nabla\boldsymbol{v}+\nabla\boldsymbol{v}^T\left(\nabla\boldsymbol{\tau}^{\boldsymbol{u}}\right)^{-T}\right]\big)\Big)\cdot$$

$$\cdot\,\tilde{\boldsymbol{n}}\left(\boldsymbol{\tau}^{\boldsymbol{u}}\left(\boldsymbol{x}\right)\right)\left|\det J_{\boldsymbol{\tau}^{\boldsymbol{u}}}\left(\boldsymbol{x}\right)\right|\mathrm{d}S+m\boldsymbol{g}+\boldsymbol{f}_{\mathrm{ext}},$$

$$\boldsymbol{m}\left(\left(\boldsymbol{v},p^*,\alpha\right),\boldsymbol{u}\right)=\int_{\Gamma_{\mathrm{ref,B}}}\Bigg\{\left(\boldsymbol{\tau}^{\boldsymbol{u}}\left(\boldsymbol{x}\right)-\boldsymbol{\tau}^{\boldsymbol{u}}\left(\boldsymbol{x}_G\right)\right)\times\Big(\Big[\left(p^*+\rho\boldsymbol{g}^T\boldsymbol{\tau}^{\boldsymbol{u}}\left(\boldsymbol{x}\right)\right)\boldsymbol{I}$$

$$-\mu_{\mathrm{eff}}\Big\{\left(\nabla\boldsymbol{\tau}^{\boldsymbol{u}}\right)^{-1}\nabla\boldsymbol{v}+\nabla\boldsymbol{v}^T\left(\nabla\boldsymbol{\tau}^{\boldsymbol{u}}\right)^{-T}\Big\}\Big]\tilde{\boldsymbol{n}}(\boldsymbol{\tau}^{\boldsymbol{u}}\left(\boldsymbol{x}\right))\Big)\Bigg\}\left|\det J_{\boldsymbol{\tau}^{\boldsymbol{u}}}\left(\boldsymbol{x}\right)\right|\mathrm{d}S$$

$$+\left(\boldsymbol{\tau}^{\boldsymbol{u}}\left(\boldsymbol{x}_{\mathrm{ext}}\right)-\boldsymbol{\tau}^{\boldsymbol{u}}\left(\boldsymbol{x}_G\right)\right)\times\boldsymbol{f}_{\mathrm{ext}},$$

so that

(3.26)

$$\boldsymbol{f}_{\boldsymbol{u}}\left(\left(\boldsymbol{v},p^*,\alpha\right),\boldsymbol{u}\right)^T=\int_{\Gamma_{\mathrm{ref,B}}}\Bigg\{\Bigg(\Bigg[\tilde{\boldsymbol{n}}\left(\boldsymbol{\tau}^{\boldsymbol{u}}\left(\boldsymbol{x}\right)\right)^T\Big(\rho\boldsymbol{g}^T\frac{\partial}{\partial u_i}\left(\boldsymbol{\tau}\left(\boldsymbol{x}\right)\right)\boldsymbol{I}$$

$$-\mu_{\mathrm{eff}}\left(\frac{\partial}{\partial u_i}\left(\nabla\boldsymbol{\tau}^{\boldsymbol{u}}\right)^{-1}\nabla\boldsymbol{v}+\nabla\boldsymbol{v}^T\frac{\partial}{\partial u_i}\left(\nabla\boldsymbol{\tau}^{\boldsymbol{u}}\right)^{-T}\right)\Big)\Bigg]_{i=1}^n+\nabla_{\boldsymbol{u}}\left(\tilde{\boldsymbol{n}}\left(\boldsymbol{\tau}^{\boldsymbol{u}}\left(\boldsymbol{x}\right)\right)\right)\cdot$$

$$\cdot\left(\left(p^*+\rho\boldsymbol{g}^T\boldsymbol{\tau}^{\boldsymbol{u}}\left(\boldsymbol{x}\right)\right)\boldsymbol{I}-\mu_{\mathrm{eff}}\big(\left(\nabla\boldsymbol{\tau}^{\boldsymbol{u}}\right)^{-1}\nabla\boldsymbol{v}+\nabla\boldsymbol{v}^T\left(\nabla\boldsymbol{\tau}^{\boldsymbol{u}}\right)^{-T}\big)\right)\Bigg)\left|\det J_{\boldsymbol{\tau}^{\boldsymbol{u}}}\left(\boldsymbol{x}\right)\right|$$

$$+\operatorname{sgn}\left(\det J_{\boldsymbol{\tau}^{\boldsymbol{u}}}\left(\boldsymbol{x}\right)\right)\left[\operatorname{tr}\left(\operatorname{adj}\left(\nabla\boldsymbol{\tau}^{\boldsymbol{u}}\right)\frac{\partial}{\partial u_i}\left(\nabla\boldsymbol{\tau}^{\boldsymbol{u}}\right)\right)\right]_{i=1}^n\tilde{\boldsymbol{n}}\left(\boldsymbol{\tau}^{\boldsymbol{u}}\left(\boldsymbol{x}\right)\right)^T\cdot$$

$$\cdot \Big(\big(p^* + \rho \boldsymbol{g}^T \boldsymbol{\tau}^{\boldsymbol{u}}(\boldsymbol{x})\big) \boldsymbol{I} - \mu_{\text{eff}} \Big((\nabla \boldsymbol{\tau}^{\boldsymbol{u}})^{-1} \nabla \boldsymbol{v} + \nabla \boldsymbol{v}^T (\nabla \boldsymbol{\tau}^{\boldsymbol{u}})^{-T} \Big) \Big) \Big\} \mathrm{d}S$$

(3.27)

$$\begin{aligned}
\boldsymbol{m}_{\boldsymbol{u}}\left((\boldsymbol{v}, p^*, \alpha), \boldsymbol{u}\right)^T = \int_{\Gamma_{\text{ref,B}}} & \Bigg[\Bigg[\Big[\Big(\frac{\partial}{\partial u_i} \boldsymbol{\tau}^{\boldsymbol{u}}(\boldsymbol{x}) - \frac{\partial}{\partial u_i} \boldsymbol{\tau}^{\boldsymbol{u}}(\boldsymbol{x}_G) \Big) \times \\
& \times \Big(\Big(\big(p^* + \rho \boldsymbol{g}^T \boldsymbol{\tau}^{\boldsymbol{u}}(\boldsymbol{x})\big) \boldsymbol{I} - \mu_{\text{eff}} \big((\nabla \boldsymbol{\tau}^{\boldsymbol{u}})^{-1} \nabla \boldsymbol{v} + \nabla \boldsymbol{v}^T (\nabla \boldsymbol{\tau}^{\boldsymbol{u}})^{-T} \big) \Big) \tilde{\boldsymbol{n}} (\boldsymbol{\tau}^{\boldsymbol{u}}(\boldsymbol{x})) \Big) \Big]^T \Bigg]_{i=1}^n \\
& + \Bigg[\Big((\boldsymbol{\tau}^{\boldsymbol{u}}(\boldsymbol{x}) - \boldsymbol{\tau}^{\boldsymbol{u}}(\boldsymbol{x}_G)) \times \Big(- \mu_{\text{eff}} \Big(\frac{\partial}{\partial u_i} (\nabla \boldsymbol{\tau}^{\boldsymbol{u}})^{-1} \nabla \boldsymbol{v} + \nabla \boldsymbol{v}^T \frac{\partial}{\partial u_i} (\nabla \boldsymbol{\tau}^{\boldsymbol{u}})^{-T} \Big) \tilde{\boldsymbol{n}} (\boldsymbol{\tau}^{\boldsymbol{u}}(\boldsymbol{x})) \\
& \quad + \Big(\big(p^* + \rho \boldsymbol{g}^T \boldsymbol{\tau}^{\boldsymbol{u}}(\boldsymbol{x})\big) \boldsymbol{I} - \mu_{\text{eff}} \big((\nabla \boldsymbol{\tau}^{\boldsymbol{u}})^{-1} \nabla \boldsymbol{v} + \nabla \boldsymbol{v}^T (\nabla \boldsymbol{\tau}^{\boldsymbol{u}})^{-T} \big) \Big) \cdot \\
& \qquad \cdot \frac{\partial}{\partial u_i} \tilde{\boldsymbol{n}} (\boldsymbol{\tau}^{\boldsymbol{u}}(\boldsymbol{x})) \Big) \Big)^T \Bigg]_{i=1}^n \Bigg] \left| \det J_{\boldsymbol{\tau}^{\boldsymbol{u}}}(\boldsymbol{x}) \right| \\
& + \operatorname{sgn} (\det J_{\boldsymbol{\tau}^{\boldsymbol{u}}}(\boldsymbol{x})) \Big(\operatorname{tr} \Big(\operatorname{adj} (\nabla \boldsymbol{\tau}^{\boldsymbol{u}}) \frac{\partial}{\partial u_i} (\nabla \boldsymbol{\tau}^{\boldsymbol{u}}) \Big) \Big)_{i=1}^n \cdot \Big[(\boldsymbol{\tau}^{\boldsymbol{u}}(\boldsymbol{x}) - \boldsymbol{\tau}^{\boldsymbol{u}}(\boldsymbol{x}_G)) \times \\
& \times \Big(\Big(\big(p^* + \rho \boldsymbol{g}^T \boldsymbol{\tau}^{\boldsymbol{u}}(\boldsymbol{x})\big) \boldsymbol{I} - \mu_{\text{eff}} \big((\nabla \boldsymbol{\tau}^{\boldsymbol{u}})^{-1} \nabla \boldsymbol{v} + \nabla \boldsymbol{v}^T (\nabla \boldsymbol{\tau}^{\boldsymbol{u}})^{-T} \big) \Big) \tilde{\boldsymbol{n}} (\boldsymbol{\tau}^{\boldsymbol{u}}(\boldsymbol{x})) \Big) \Big]^T \mathrm{d}S \\
& + \Bigg[\Big(\Big(\frac{\partial}{\partial u_i} \boldsymbol{\tau}^{\boldsymbol{u}}(\boldsymbol{x}_{\text{ext}}) - \frac{\partial}{\partial u_i} \boldsymbol{\tau}^{\boldsymbol{u}}(\boldsymbol{x}_G) \Big) \times \boldsymbol{f}_{\text{ext}} \Big)^T \Bigg]_{i=1}^n .
\end{aligned}$$

This concludes the calculation of all terms required for our general approach outlined at the beginning of this section.

4. Numerical Experiments.

Now we report on our numerical experiments.

4.1. Discretization.

The discretization of the partial differential equations of this work is carried out by means of the *finite volume method*. For the multiphase calculations the phase fraction equation is solved using the *Multidimensional Universal Limiter with Explicit Solution (MULES)* algorithm [25], where an additional artificial compression term is introduced into the phase fraction equation in order to keep the interface sharp. Moreover, the primal equations are decoupled with the well-known schemes SIMPLE [22] and PISO [15] where the latter one is also adapted to be used for our adjoint equations (for details see [27]). The implementation is realized with the software library OpenFOAM® [11, 23] which is an open source software toolbox especially for CFD.

4.2. Validation.

We start by showing some numerical experiments in order to validate both the derivation of the equations as well as our implementation in the following cases:

- calculation of single- or multiphase adjoint flow fields,
- evaluation of the adjoint gradients and validation with finite differences.

Of course, we have also performed several tests for validating the primal flow calculations, [27]. We consider different test cases, namely

- NACA0012 single phase: single phase flow around a NACA0012 hydrofoil;
- Box multiphase: two phase flow around a box;
- KCS multiphase: two phase flow around the KCS ship, [20].

4.2.1. Adjoint Flow Fields.

NACA0012 single phase. We start with the single phase flow around the well-known NACA0012 profile using the drag (x-force) as objective function for deriving the adjoint system. This objective function leads to a boundary condition at the hydrofoil boundary Γ_{B} with the adjoint velocity specified by the unit vector in x-direction (see §3.2). A typical result is shown in Figure 4.1 indicating the expected behavior of the adjoint velocity having the opposite direction as the primal flow field.

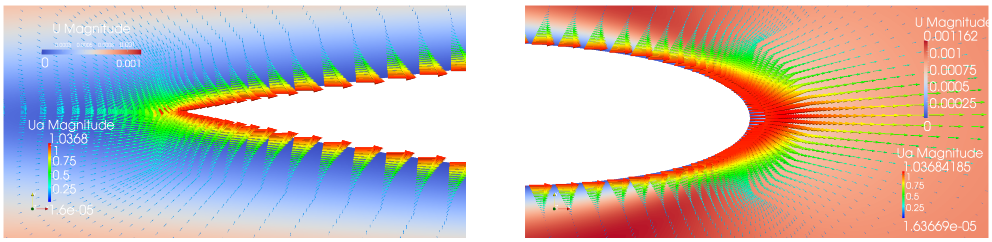

Fig. 4.1: Adjoint velocity vectors adapting to the adjoint boundary condition in the vicinity of the leading (right) and trailing (left) edge of the hydrofoil.

Multiphase box. Next, we consider the two-phase flow around a rigid box. This case has also been validated by experiments at Voith, Heidenheim, [27]. For stabilization purposes, we neglected some cross-coupling terms, see [27] for details. We use the multidimensional objective function consisting of z-forces and y-moments. The tests were performed for two different parameter combinations. The first one corresponds to the initial parameter combination for the optimization algorithm, namely a trim angle of 0° and a sinkage of 0 mm, and the second parameter combination is located close to the optimum (4°, -11mm). The residual plot in Figure 4.2 shows fast convergence using the mentioned stabilization. We stopped at a residual below 10^{-8}.

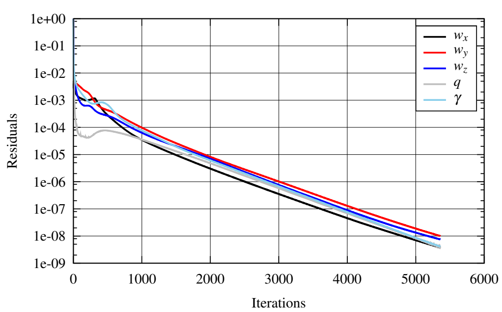

Fig. 4.2: Box: Example of residuals for the segregated multiphase adjoint equations in the iterative solution process (4°, -11 mm).

Figure 4.3 shows the adjoint velocity field (glyphs) adapting to the boundary condition resulting from the objective functions. The symmetry plane of the computational domain is colored by the adjoint phase fraction. Some high velocity values appear at the edges of the box, which could possibly affect the accuracy of the gradients. This will be validated in the next section. Figure 4.4 shows the adjoint pressures

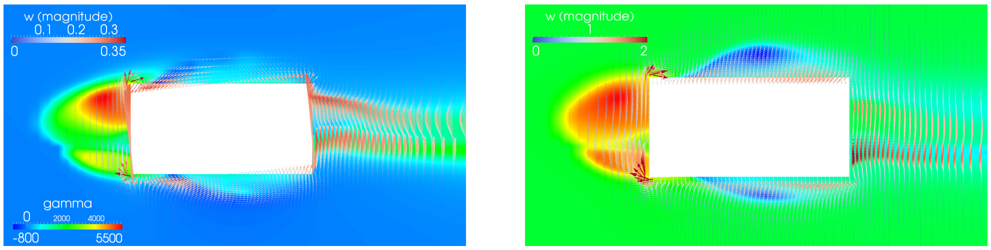

Fig. 4.3: Box: Adjoint velocity field (glyphs) and adjoint phase fraction (background) in the vicinity of the box for the y-moment (left) and the z-force (right).

for the two objective functions.

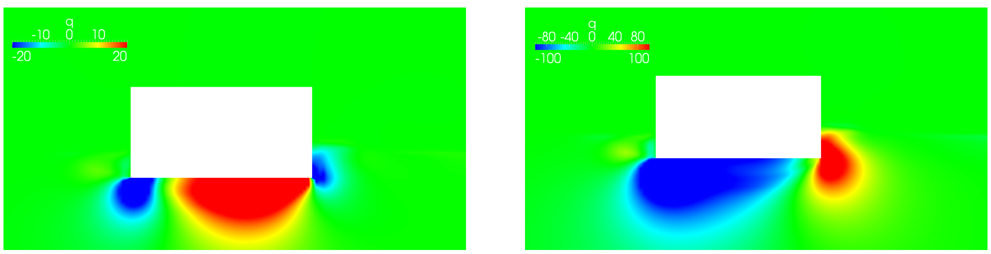

Fig. 4.4: Box: Adjoint pressure in the vicinity of the box for the y-moment (left) and the z-force (right).

KCS multiphase. For the KCS ship we used the y-moment objective function and the hydrostatic equilibrium position with a trim angle of 0° and a sinkage of 0 mm. Employing the modifications in the cross-coupling terms mentioned above, stable and fast convergence of the adjoint system could be achieved, as we can see in the residual plot in Figure 4.5. The stopping criterion was residual below 10^{-8}.

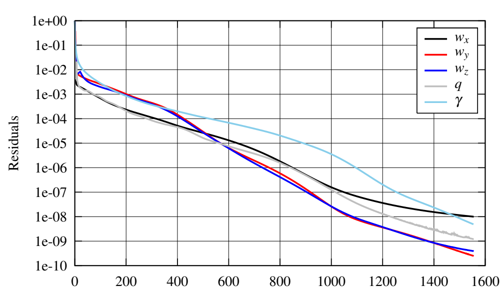

Fig. 4.5: KCS: Residuals of the segregated multiphase adjoint equations in the iterative solution process (0°, 0 mm).

Figure 4.6 shows the adjoint flow fields for adjoint phase fraction, adjoint velocity magnitude and adjoint pressure in the symmetry plane of the ship.

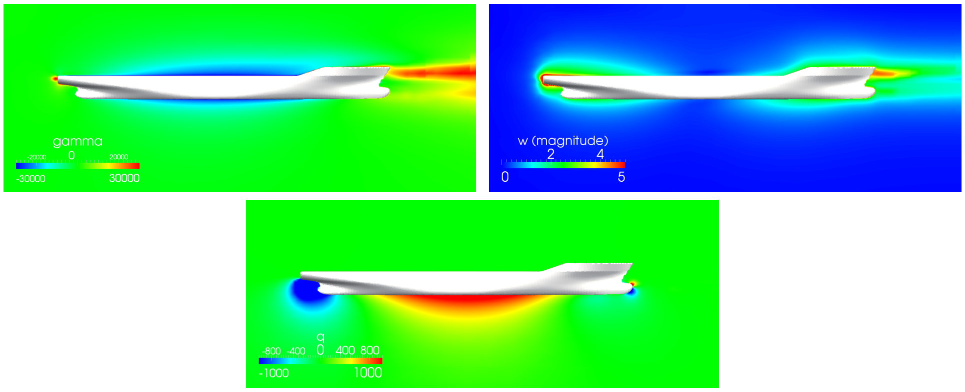

Fig. 4.6: KCS: Adjoint phase fraction for y-moment (top left), adjoint velocity for y-moment (top right) and adjoint pressure for y-moment (bottom).

4.2.2. Adjoint Gradient. Next, we test the computation of the adjoint gradient and use two variants of finite differences for the validation. By "FD" we indicate a standard finite difference approximation of the adjoint gradient. The second variant is based upon the splitting

$$j'(\boldsymbol{u})[\delta \boldsymbol{u}] = \underbrace{\mathcal{J}_{\boldsymbol{u}}(\boldsymbol{y}(\boldsymbol{u}), \boldsymbol{u})[\delta \boldsymbol{u}]}_{(1)} + \underbrace{\mathcal{J}_{\boldsymbol{y}}(\boldsymbol{y}(\boldsymbol{u}), \boldsymbol{u})\, \boldsymbol{y}'(\boldsymbol{u})[\delta \boldsymbol{u}]}_{(2)},$$

into the explicit dependency on $\boldsymbol{u}$ (1) and the implicit dependency in $\boldsymbol{y}(\boldsymbol{u})$ (2), where only (2) is approximated by finite differences, whereas (1) can be directly evaluated with the transformation approach (see §3.3.2). This method is indicated as "SemiFD" and allows us to separately validate the two components of the adjoint gradient.

NACA0012 single-phase. We used the non-dimensionalized drag as objective function, i.e., the quotient of the forces (divided by the density) and the term $\frac{1}{2}\boldsymbol{v}_{\text{in}}^2 A = \frac{1}{2} \cdot 0.33^2 \cdot 0.5 = 0.02723$. The evaluations were performed for parameter values in the range of $0°$ to $10.5°$ with increments of $0.5°$. The results for the drag coefficient and the three gradient alternatives for the selected validation range of $4.5°$ to $9.5°$ are illustrated in Figure 4.7.

It can be observed that the SemiFD values are very close to the values of the FD calculation and the adjoint gradient value is a little bit below. This is reasonable as the FD and SemiFD approximations have the same order of accuracy. Moreover, finite differences over-predict the gradient for functions with increasing slope. As the values for FD and SemiFD are almost the same we can also conclude that the computation of the explicit term (1) is correct.

Box multiphase. The adjoint gradients for multiphase flow are evaluated using (3.25)-(3.27) with the derivatives for a whole-grid transformation. Using this transformation approach we observe that for derivatives w.r.t. translational directions nearly all terms containing adjoint flow variables vanish as $\frac{\partial}{\partial u_i}(\nabla_{\boldsymbol{x}} \boldsymbol{\tau}(\boldsymbol{x}, \boldsymbol{u})) = 0$ for $i = 4, 5, 6$. The parts that remain are terms that only exist in the artificial transition area of the interface between water and air. As already mentioned in Remark 3.6,

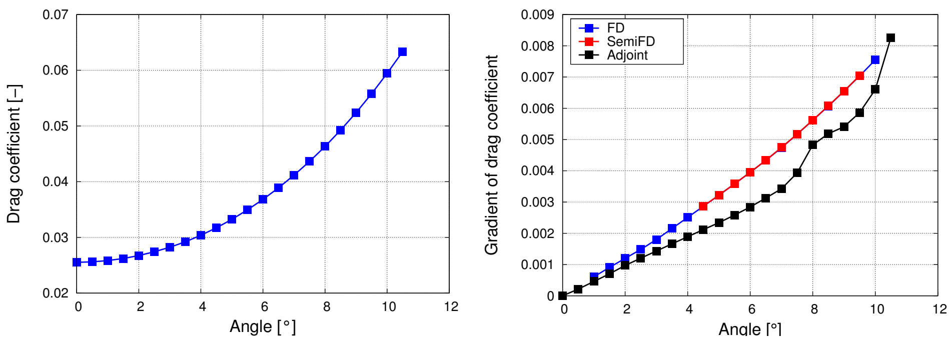

Fig. 4.7: NACA0012 gradient; left: drag coefficient, right: gradient of the drag.

these terms cannot be evaluated accurately and are therefore neglected. This speeds up the computation as only an adjoint system for the y-moment needs to be solved.

We used the parameters (0°, 0 mm) and (4°, -11 mm). For the first parameter we also performed FD calculations with disturbances of 0.2° and -0.2 mm. We have four different relevant derivatives resulting from two different objective function components (y-moment and z-force) and two parameters considered (trim and sinkage, denoted by u_2 and u_6). Note, that the main influence on the y-moment results from the trim angle and the main influence on the z-force results from the sinkage. Therefore the validations were performed for these derivatives $\frac{\partial j_i(\boldsymbol{u})}{\partial u_i}$, $i \in \{2, 6\}$. Figure 4.8a shows the convergence for the adjoint derivative of the y-moment w.r.t. the second parameter, the corresponding values are given in Table 4.1.

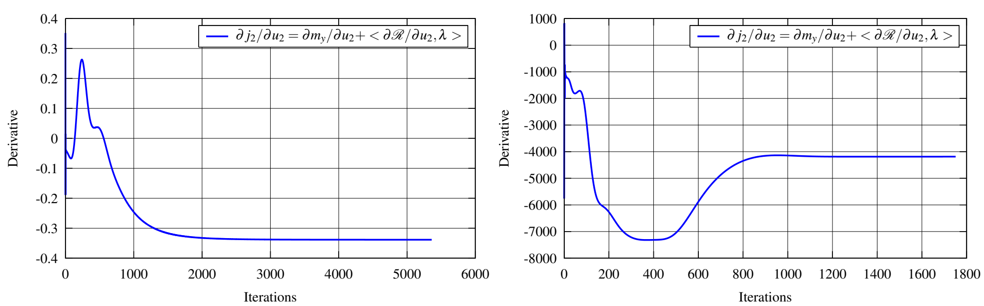

(a) Box: w.r.t. (4°, -11 mm).

(b) KCS: w.r.t. (0°, 0 mm).

Fig. 4.8: Convergence of the adjoint derivatives of the y-moment.

u_2	u_6	$\frac{\partial j_2(\boldsymbol{u})}{\partial u_2}$ (FD)	$\frac{\partial j_2(\boldsymbol{u})}{\partial u_2}$ (SemiFD)	$\frac{\partial j_2(\boldsymbol{u})}{\partial u_2}$ (Adjoint)
0°	0 mm	-0.328	-0.344 (+4.6%)	-0.329 (+0.3%)
4°	-11 mm	-0.365	-0.360 (-8.9%)	-0.338 (-7.4%)

Table 4.1: Box: Multiphase derivative validation for $\frac{\partial j_2(\boldsymbol{u})}{\partial u_2}$.

For $\frac{\partial j_6(\boldsymbol{u})}{\partial u_6}$, the terms existing only in the artificial transition area of the interface between water and air are neglected. Therefore we analyze if the accuracy is still acceptable. In Table 4.2 the results are compared with the FD derivative. The approximations are quite good so that we use this approach for all subsequent computations.

u_2	u_6	$\frac{\partial j_6(\boldsymbol{u})}{\partial u_6}$ (FD)	$\frac{\partial j_6(\boldsymbol{u})}{\partial u_6}$ (Adjoint)
0°	0 mm	-1.064	-0.978 (-8.0%)
4°	-11 mm	-1.013	-0.985 (-2.8%)

Table 4.2: Box: Multiphase derivative validation for $\frac{\partial j_6(\boldsymbol{u})}{\partial u_6}$.

KCS multiphase. For the KCS we use the parameter combination (0°, 0 mm), as this is the initial value for the optimization algorithm. The values of $\frac{\partial j_2(\boldsymbol{u})}{\partial u_2}$ are presented in Figure 4.8b. Convergence is attained within about 1.000 iterations, which has to be compared with the primal flow simulations using $T = 100s$ with about 100.000 iterations. Thus, the overhead due to the adjoint approach is almost negligible.

In Table 4.3, the comparison with the finite difference approximations are shown. We observe deviations below 20% which –for derivatives– we consider as good.

u_2	u_6	$\frac{\partial j_2(\boldsymbol{u})}{\partial u_2}$ (FD)	$\frac{\partial j_2(\boldsymbol{u})}{\partial u_2}$ (SemiFD)	$\frac{\partial j_2(\boldsymbol{u})}{\partial u_2}$ (Adjoint)
0°	0 mm	-3.551	-3.906 (+10.0%)	-4.188 (+17.9%)
0.05°	0 mm	-3.159	-3.283 (+3.9%)	-3.333 (+5.5%)
0.05°	-10 mm	-3.360	-3.337 (-0.7%)	-4.012 (+19.4%)

Table 4.3: KCS: Multiphase derivative validation for $\frac{\partial j_2(\boldsymbol{u})}{\partial u_2}$.

The results for $\frac{\partial j_6(\boldsymbol{u})}{\partial u_6}$ are presented in Table 4.4. Although the contributions of the artificial transition area of the fluid interface were again neglected, the deviations are less than 6% which is by all means sufficiently accurate.

u_2	u_6	$\frac{\partial j_6(\boldsymbol{u})}{\partial u_6}$ (FD)	$\frac{\partial j_6(\boldsymbol{u})}{\partial u_6}$ (Adjoint)
0°	0 mm	-58.779	-61.923 (+5.4%)
0.05°	0 mm	-59.996	-60.597 (+2.3%)
0.05°	-10 mm	-59.979	-60.597 (+1.0%)

Table 4.4: KCS: Multiphase derivative validation for $\frac{\partial j_6(\boldsymbol{u})}{\partial u_6}$.

4.3. Gradient-based Optimization. Next, we present our results for the gradient-based optimization. We also validate our numerical realization in terms of finite differences. We use the same test cases as for the validation above.

NACA0012 single case. We aim at determining the angle of attack (rotation around the z-axis) that minimizes the drag coefficient (which is a similar setup as forces minimization for ship motion, see below), i.e., the objective function is given by

$$j(\boldsymbol{u}) = c_D(\boldsymbol{u}) = \frac{f_x(\boldsymbol{y}(\boldsymbol{u}), \boldsymbol{u})}{\frac{1}{2}\rho \|\boldsymbol{v}\|^2 A}, \qquad \text{with parameter } \boldsymbol{u} = u_3 = \psi.$$

In order to optimize, we use a gradient descent scheme. The initial parameter value was set to $\psi^{(0)} = u_3^{(0)} := 10°$. The gradient was calculated by the adjoint approach for the objective function $\rho^{-1} f_x(\boldsymbol{y}(u), u)$, which was later non-dimensionalized by the factor $2\|\boldsymbol{v}\|^{-2} A^{-1}$. The stopping criterion was set as $|j(u^{(k)}) - j(u^*)| < 10^{-6}$, where u^* is the optimal solution that is known to be $u^* = 0$ with $j(u^*) = 0.0255289$.

The results for a fixed step size $0.5s$ as well as for an Armijo search are shown in Figure 4.9. we observe convergence which, however, is not guaranteed by the theory. For the line search, the step in iteration 1 and 2 is rejected once, whereas for the initial and last step the Armijo criterion is directly fulfilled.

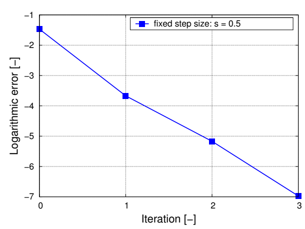

Fig. 4.9: NACA0012: Convergence with fixed step size ($s = 0.5$).

Box multiphase. For this case, we search the multidimensional root of the y-moment and the z-force and determine the corresponding trim angle and sinkage value. Thus, in these test cases the objective function is given by

$$j(\boldsymbol{u}) = \begin{pmatrix} m(\boldsymbol{y}(\boldsymbol{u}), \boldsymbol{u}) \\ f(\boldsymbol{y}(\boldsymbol{u}), \boldsymbol{u}) \end{pmatrix} \quad \text{with the parameter } \boldsymbol{u} = \begin{pmatrix} u_2 \\ u_6 \end{pmatrix} = \begin{pmatrix} \theta \\ \Delta z \end{pmatrix}.$$

Here, we perform a multidimensional root search using Newton's method instead of a minimization as in the single-phase case (which is beneficial due to the almost linear dependence of the components of j w.r.t. their respective dominating parameters). The corresponding Jacobian and its inverse can easily be computed. Moreover, there is an additional output functional of interest, namely the resistance $f_x(\boldsymbol{y}(\boldsymbol{u}), \boldsymbol{u})$ of the ship.

It turns out that the Newton iterations require only *one* additional adjoint calculation since $\frac{\partial m_y}{\partial u_6}$ and $\frac{\partial f_z}{\partial u_6}$ can be evaluated using primal flow fields only. The results of the Newton iterations for some alternatives are presented in Figure 4.10.

After only one iteration the output value of the resistance is already accurate up to 0.5% accuracy. The values for trim and sinkage are less accurate with 7.1% and 14.5% deviation. However, with the second iteration this deviation already reduces to under 3% in both cases.

As mentioned above the dependency on the main parameter component is almost linear and therefore the respective derivative values for $\frac{\partial}{\partial u_2} m_y$ and $\frac{\partial}{\partial u_6} f_z$ do not change much during the iterations. Hence, in further iterations the derivative values calculated accurately in the initial iteration are reused. This means that the additional

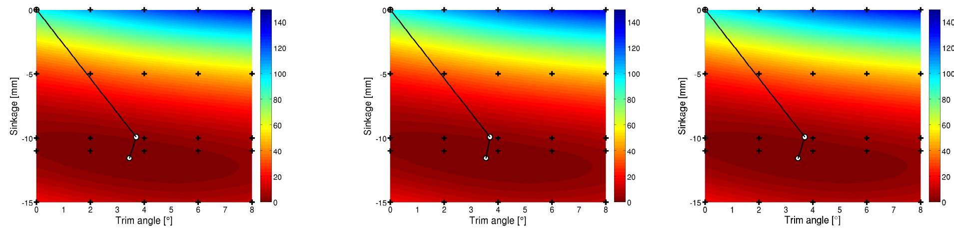

Fig. 4.10: Box: Convergence of Newton iterations using adjoint derivatives in the initial iteration and finite differences derivatives in further iterations with the previous parameter as approximation (left), using adjoint derivatives in all iterations and the previous parameter as approximation (center) and using adjoint derivatives in the initial iteration and old derivative values in further iterations with the previous parameter as approximation (right) (background color: quadratic error).

accuracy of the parameters is achieved without further effort. The results of this strategy are shown in Figure 4.10.

KCS multiphase. We use the same approach as in the box multiphase case above. The stopping criterion was again set to $\|j(\boldsymbol{u}^{(k)})\|_2^2 \, \|j(\boldsymbol{u}^{(0)})\|_2^{-2} < 3.0 \cdot 10^{-2}$. The results are shown in Figure 4.11.

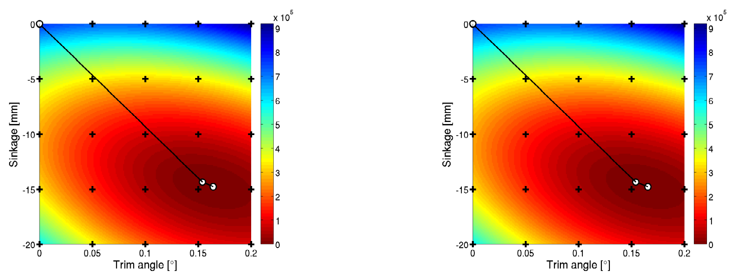

Fig. 4.11: KCS: Convergence of Newton iterations using adjoint derivatives in the initial iteration, old derivative values in further iterations and the previous parameter as approximation (left) and using adjoint derivatives in all iterations and the previous parameter as approximation (right) (color: quadratic error).

After only one iteration we obtain very accurate resistance results (f_x) that are within the accuracy of the dynamic oscillations of a time-resolved reference computation (equations of motion). Using the additional evaluation for the parameter values of the next iteration (without the corresponding flow solution) the trim and sinkage parameter values are equally accurate. As already observed in the adjoint gradient validation of §4.2.2 the value of $\frac{\partial}{\partial u_2} m_y$ for 0° and 0 mm is slightly over-estimated, which results in a value for $u_2^{(1)}$ that is further away from the final value than in a corresponding finite differences calculation. However, even if this value is reused for the parameter evaluation at iteration 1, the value $u_2^{(2)}$ already has a deviation of under 1%. Furthermore, especially for this test case with a real ship the effort for the adjoint calculation is very low in comparison to static flow calculations of the ship.

Therefore even performing a new adjoint derivative calculation does not have a major impact on the overall efficiency.

These results clearly show that we are able to calculate the resistance of a ship considering trim and sinkage with only one additional static flow calculation and one or two adjoint evaluations depending on the required accuracy. Moreover, in comparison to dynamic calculations, static calculations are more robust and therefore need fewer inner iterations per outer iteration and the adjoint can be solved at an expense that is negligible as compared to primal computations.

5. Summary and Outlook. We observe an extremely fast numerical scheme for solving the rigid body motion in a two-phase flow. The overhead of the adjoint computations is almost negligible compared to the flow simulation which means that the *full* pde-constraint optimization problem can be solved with the complexity of about *two* static flow simulation (one for the initial position at the construction waterline equally needed for the dynamic calculation via equations of motion and one additional static computation in the optimization).

Since all equations are completely detailed, corresponding simulations can immediately be done for other rigid bodies as well, which we already did for a variety of real ship geometries.

REFERENCES

[1] F. Abergel and R. Temam, *On some control problems in fluid mechanics*, Theoretical and Computational Fluid Dynamics, 1 (1990), pp. 303–325.

[2] R. Azcueta, *Computation of turbulent free-surface flows around ships and floating bodies*, PhD thesis, Technical University of Hamburg-Harburg, 2001.

[3] J. U. Brackbill, D. B. Kothe, and C. Zemach, *A continuum method for modeling surface tension*, J. Comput. Phys., 100 (1992), pp. 335–354.

[4] C. Brandenburg, *Adjoint-Based Adaptive Multilevel Shape Optimization based on Goal-Oriented Error Estimators for the Instationary Navier-Stokes Equations*, PhD thesis, Technische Univertität Darmstadt, 2011.

[5] C. Brandenburg, F. Lindemann, M. Ulbrich, and S. Ulbrich, *Advanced Numerical Methods for PDE Constrained Optimization with Application to Optimal Design in Navier Stokes Flow*, in Constrained Optimization and Optimal Control for Partial Differential Equations, G. Leugering, S. Engell, A. Griewank, M. Hinze, R. Rannacher, V. Schulz, M. Ulbrich, and S. Ulbrich, eds., vol. 160 of International Series of Numerical Mathematics, Springer Basel, 2012, pp. 257–275.

[6] R. P. Dwight and J. Brezillion, *Effect of Approximations of the Discrete Adjoint on Gradient-Based Optimization*, AIAA Journal, 44 (2006), pp. 3022–3031.

[7] J. H. Ferziger and M. Perić, *Computational Methods for Fluid Dynamics*, Springer London, Limited, 2002.

[8] M. B. Giles and N. A. Pierce, *An Introduction to the Adjoint Approach to Design*, Flow, Turbulence and Combustion, 65 (2000), pp. 393–415.

[9] W. J. Gordon and C. A. Hall, *Construction of curvilinear co-ordinate systems and applications to mesh generation*, Internat. J. Numer. Methods Engrg., 7 (1973), pp. 461–477.

[10] ———, *Transfinite element methods: blending-function interpolation over arbitrary curved element domains*, Numer. Math., 21 (1973/74), pp. 109–129.

[11] OpenCFD Ltd (ESI Group), *OpenFOAM® - The OpenSource Computational Fluid Dynamics (CFD) Toolbox*. `http://www.openfoam.com/`, 2013.

[12] M. Hinze, *Optimal and instantaneous control of the instationary Navier-Stokes equations*, habilitation thesis, Technische Univertität Berlin, 2000.

[13] C. W. Hirt, A. A. Amsden, and J. L. Cook, *An arbitrary Lagrangian-Eulerian computing method for all flow speeds*, Journal of Computational Physics, 14 (1974), pp. 227–253.

[14] C. W. Hirt and B. D. Nichols, *Volume of Fluid (VOF) Method for the Dynamics of Free Boundaries*, J. Comput. Phys., 39 (1981), pp. 201–225.

[15] R. I. Issa, *Solution of the implicitly discretised fluid flow equations by operator-splitting*, J. Comput. Phys., 62 (1986), pp. 40–65.

[16] W. P. Jones and B. E. Launder, *The prediction of laminarization with a two-equation model of turbulence*, International Journal of Heat and Mass Transfer, 15 (1972), pp. 301–314.

[17] C. G. Kyriakos, Dimitrios I. P., Evangelos M. P.-K., and Carsten O., *Adjoint Methods in CFD-Based Optimization - Gradient Computation & Beyond*, in CD-ROM Proceedings of the 6th European Congress on Computational Methods in Applied Sciences and Engineering (ECCOMAS 2012), September 10-14, 2012, Vienna, Austria, J. Eberhardsteiner, H. J. Böhm, and F. G. Rammerstorfer, eds., Vienna University of Technology, Austria, September 2012.

[18] J. Lee, S.J. Lee, and S.H. Van, *Wind tunnel test on a double deck shaped ship model*, in 3rd International Conference on Hydrodynamics, Seoul, Korea, 1998.

[19] F. Menter, M. Kuntz, and R. Langtry, *Ten years of Industrial experience with the SST model*, in Turbulence, Heat and Mass Transfer 4, K. Hanjalić, Y. Nagano, and M. Tummers, eds., 2003.

[20] Korea Research Institute of Ships and Ocean Engineering (KRISO), *KRISO container ship (KCS), geometry*, last access: 14.06.2014. `http://www.nmri.go.jp/institutes/fluid_performance_evaluation/cfd_rd/cfdws05/Detail/KCS/kcs_g&c.htm`.

[21] C. Othmer, *A continuous adjoint formulation for the computation of topological and surface sensitivities of ducted flows*, Internat. J. Numer. Methods Fluids, 58 (2008), pp. 861–877.

[22] S. V. Patankar and D. B. Spalding, *A Calculation Procedure for Heat, Mass and Momentum Transfer in Three-Dimensional Parabolic Flows*, Int. J. Heat Mass Transfer, 15 (1972), pp. 1787–1972.

[23] S. Petropoulou, *Industrial Optimisation Solutions Based on OpenFOAM® Technology*, in Proceedings of the V European Conference on Computational Fluid Dynamics ECCOMAS CFD 2010 J. C. F. Pereira, A. Sequeira and J. M. C. Pereira (Eds) Lisbon, Portugal,14-17 June 2010, 2010.

[24] L. Prandtl, *Über Flüssigkeitsbewegung bei sehr kleiner Reibung*, in Verhandlungen des dritten internationalen Mathematiker-Kongresses, A. Krazer, ed., Teubner, 1904, pp. 484–491.

[25] H. Rusche, *Computational fluid dynamics of dispersed two-phase flows at high phase fractions*, PhD thesis, Imperial College (London), 2002.

[26] O. Soto and R. Löhner, *On the Boundary Computation of Flow Sensitivities*, in 42nd AIAA Aerospace Sciences Meeting and Exhibit, American Institute of Aeronautics and Astronautics, 2004.

[27] J. Springer, *Multiphase Adjoint Optimization for Efficient Calculation of Rigid Body Positions in Navier-Stokes Flow*, PhD thesis, Univertität Ulm, 2014.

[28] A. Stück, *Adjoint Navier-Stokes methods for hydrodynamic shape optimisation*, PhD thesis, Inst. for Fluid Dynamics and Ship Theory, November 2011.

[29] D. Thévenin and G. Janiga, eds., *Optimization and Computational Fluid Dynamics*, Springer-Verlag, Berlin, 2008.

[30] J. F. Thompson, Z. U. A. Warsi, and C. W. Mastin, *Numerical grid generation*, North-Holland Publishing Co., New York, 1985. Foundations and applications.

[31] M. Ulbrich, *Constrained optimal control of Navier-Stokes flow by semismooth Newton methods*, Systems & Control Letters, 48 (2003), pp. 297–311.

[32] Y. Xing-Kaeding, *Unified Approach to Ship Seakeeping and Maneuvering by a RANSE Method*, Arbeitsbereiche Schiffbau, TU Hamburg-Harburg, 2006.

[33] D. Xiu and D. M. Tartakovsky, *Numerical methods for differential equations in random domains*, SIAM J. Sci. Comput., 28 (2006), pp. 1167–1185 (electronic).